



UNIVERSIDADE
E D U A R D O
MONDLANE

FACULTY OF ENGINEERING

MASTER PROGRAM IN HYDROCARBON PROCESSING ENGINEERING

**INCORPORATION OF FLARE GAS INTO METHANOL PRODUCTION:
TECHNO-ECONOMIC FEASIBILITY ON TRI-REFORMING PROCESS
MODELING, SIMULATION AND HEAT INTEGRATION**

A DISSERTATION BY

LEMOS MARTA MAHUMANE

MAPUTO

MARCH 2025



UNIVERSIDADE
E D U A R D O
MONDLANE

FACULTY OF ENGINEERING

MASTER PROGRAM IN HYDROCARBON PROCESSING ENGINEERING

**INCORPORATION OF FLARE GAS INTO METHANOL PRODUCTION:
TECHNO-ECONOMIC FEASIBILITY ON TRI-REFORMING PROCESS
MODELING, SIMULATION AND HEAT INTEGRATION**

A DISSERTATION BY

Lemos Marta Mahumane

SURPEVISOR

Prof. João Chidamoio, Eng.

MAPUTO

MARCH 2025

DECLARATION OF DOCUMENT ORIGINALITY

"I declare that this dissertation has never been submitted to obtain any degree or in any other context and is the result of my own individual work. This dissertation is presented in partial fulfillment of the requirements for the degree of Master of Science in Hydrocarbon Processing Engineering, from the Universidade Eduardo Mondlane"

Submitted by:

ABSTRACT

The primary objective of this research is to evaluate the feasibility of producing methanol using syngas obtained from methane tri-reforming, incorporating flare gas as a raw material, through techno-economic analysis. The simulation of the tri-reforming reactor utilizes kinetic model developed by Borreguero et al. (2020), while the methanol reactor simulation is based on the kinetic model developed by Bussche and Froment (1996).

A configuration involving three pre-reactors is utilized to convert the heavier hydrocarbons found in methane source raw materials. These heavier hydrocarbons could lead to catalyst deactivation in the tri-reforming reactor. Additionally, the pre-reactors are utilized to generate the energy needed for the steam reforming and dry reforming of methane reactions.

A sensitivity analysis was conducted to examine how the feed composition, pressure, and temperature affect the syngas production process. The impact of temperature was investigated by maintaining a constant pressure of 1 atm and a feed $\text{H}_2\text{O}/\text{CH}_4$ ratio of 1.5 in the methane tri-reforming reactor, while varying the temperature between 250 °C and 950 °C. The influence of pressure was assessed by maintaining a constant reactor temperature of 850 °C and a specific $\text{H}_2\text{O}/\text{CH}_4$ ratio, while varying the pressure from 1 to 10 atm. The effect of the feed $\text{H}_2\text{O}/\text{CH}_4$ molar ratio was investigated by maintaining a constant reactor temperature of 850 °C and a specific pressure, while varying the feed $\text{H}_2\text{O}/\text{CH}_4$ ratio from 0.15 to 2.

In the methanol production section, the effect of temperature was investigated by maintaining a constant pressure of 50 atm in the methanol reactor and a syngas H_2/CO molar ratio of 2.81, while varying the temperature from 200 to 400 °C. The impact of pressure was examined by keeping the reactor temperature constant at 220 °C and the syngas H_2/CO ratio at 2.81, while varying the pressure from 1 to 79 atm. The effect of the syngas H_2/CO molar ratio on reactor performance was assessed by maintaining a constant pressure of 50 atm and a temperature of 220 °C, while varying the ratio from 0.12 to 3.

The key economic parameters, such as net present value, internal rate of return, and payback period, were computed, demonstrating the economic viability of the process. Additionally, the potential energy savings resulting from the implementation of a heat energy network for the entire methanol production process were determined.

Keywords: syngas; flare gas; tri-reforming; methanol.

DEDICATION

To my parents, Marta Januário Mahumane and Jaime Covane, expressing my gratitude for their boundless love, unwavering trust, continuous support, for instilling in me the spirit of perseverance and for always believing in my abilities.

I dedicate this work!

ACKNOWLEDGEMENTS

My heartfelt appreciation goes to my supervisor, Prof. João Chidamoio, for entrusting me with this opportunity, providing unwavering support, assistance, encouragement, mentorship, and guidance in the completion of this work.

I express my gratitude to the Center of Studies in Oil and Gas Engineering and Technology (CS-OGET), led by Prof. Luís Hélder Mendes Lucas, for the priceless learning opportunities provided in Hydrocarbon Master's Program. A special acknowledgment goes to Mozambique Rovuma Venture (MRV) for generously sponsoring my scholarship. Their belief in my capabilities, support, and commitment have given me the chance to pursue my educational goals, and I am deeply thankful for their investment in my future.

To all my colleagues from the 6th edition of this Master's Program and the Coordinator Prof. Maria Eduardo, as well as to those individuals not explicitly mentioned here but who have directly or indirectly, consciously or unconsciously contributed to my education and the completion of this work:

I am sincerely thankful!

TABLE OF CONTENTS

DECLARATION OF DOCUMENT ORIGINALITY	i
ABSTRACT	ii
DEDICATION	iii
ACKNOWLEDGEMENTS	iv
TABLE OF CONTENTS	v
LIST OF ABBREVIATIONS	vii
NOMENCLATURE	viii
LIST OF FIGURES	ix
LIST OF TABLES	x
CHAPTER I.....	1
INTRODUCTION	1
1.1 Background	1
1.2 Motivation.....	3
1.3 Research problem	4
1.4. Research limitations.....	5
1.5 Research objectives.....	6
1.5.1 General objective	6
1.5.2 Specific objectives	6
CHAPTER II	7
LITERATURE VIEW	7
2.1 Introduction.....	7
2.2 Flare gas	7
2.3 Syngas production process.....	9
2.4 Overview of the methanol production process	16
2.4.1 Reaction schemes.....	18
2.4.2 Kinetic modelling	18
2.5 Reactor for methanol production	22
CHAPTER III.....	25

RESEARCH MATERIALS, METHODS AND STRATEGIES	25
3.1 Introduction.....	25
3.2 Tools for Plant simulation and economic analysis	25
3.3 Materials	27
3.4 Key parameters for methanol production process simulation.....	28
CHAPTER IV.....	30
RESULTS AND DISCUSSION.....	30
4.1 Introduction.....	30
4.2 Syngas production results	30
4.3 Methanol production results	33
4.4 Validation of the simulation process	36
4.5 Sensitivity analysis	38
4.5.1 Effect of temperature on the equilibrium TRM reactor product.....	38
4.5.2 Effect of the H ₂ O/CH ₄ ratio in the TRM reactor and pressure on the produced syngas quality	39
4.5.3 Effect of the pressure on the output of the MeOH reactor.....	41
4.5.4 Effect of the pressure on the amount of methanol vented	42
4.5.5 Effect of the temperature on the produced methanol.....	43
4.5.6 Effect of the syngas H ₂ /CO ratio on the produced methanol.....	44
4.6 Plant energy consumption and heat integration	45
4.7 Economic assessment	51
4.8 CO ₂ reduction opportunity	56
CHAPTER V.....	57
CONCLUSIONS AND RECOMMENDATIONS	57
5.1 Introduction.....	57
5.2 Conclusions.....	57
5.3 Recommendations.....	58
REFERENCES	59

LIST OF ABBREVIATIONS

AEA	Aspen Energy Analyzer
APEA	Aspen Process Economic Analyzer
BASF	Baden Aniline and Soda Factory
BR	Boletim da República
CA	Chem Analyst
CSP	Concentrating Solar Power
DRM	Dry Reforming of Methane
EDM	Electricidade de Moçambique
EIA	Energy Information Administration
ENH	Empresa Nacional de Hidrocarbonetos
GGFR	Global Gas Flaring Reduction Partnership
HEN	Heat Exchanger Network
ICI	Imperial Chemical Industries
INP	Instituto Nacional de Petróleo
IPCC	Intergovernmental Panel on Climate Change
IRR	Internal Rate of Return
ISBL	Inside Battery Limits
LPG	Liquefied Petroleum Gas
N/A	Not Applicable
NOAA	National Oceanic and Atmospheric Administration
NPV	Net Present Value
PFD	Process Flow Diagram
PFR	Plug Flow Reactor
POM	Partial Oxidation of Methane
PR	Peng-Robinson
PSA	Pressure Swing Adsorption
PSRK	Predictive Soave–Redlich–Kwong
PSV	Pressure Safety Valve
RWGS	Reverse Water Gas Shift
SRM	Steam Reforming of Methane
WGS	Water Gas Shift

NOMENCLATURE

ΔH^o	Standard enthalpy of reaction [kJ/mol]
E_{ai}	Energy of activation [kJ mol ⁻¹]
K_{DRM}	Equilibrium constant for the DRM reaction
K_{Ei}	Equilibrium constant
K_{SRM}	Equilibrium constant for the SRM reaction
K_i	Adsorption equilibrium constant [bar ⁻¹]
K_{pi}	Equilibrium constant based on partial pressures
P_c	Critical pressure [bar]
P_i	Partial pressure [bar]
T_c	Critical temperature [K]
v	Molar volume [m ³ /mol]
f_i	Partial fugacity [bar]
k_{eqWGS}	Equilibrium constant for the WGS reaction
k_i	Kinetic factor [mol s ⁻¹ bar ⁻¹]
k_i'	Reaction rate constant [mol.s ⁻¹ kPa ⁻¹]
k_i^0	Pre-exponential factor [mol.s ⁻¹ kPa ⁻¹]
r_{DRM}	Reaction rate in the DRM process [mol s ⁻¹ kg ⁻¹]
r_{SRM}	Reaction rate in the SRM process [mol s ⁻¹ kg ⁻¹]
r_i	Reaction rate per weight of catalyst [mol s ⁻¹ kg ⁻¹]
P	Total pressure [bar]
R	Gas constant (8.314) [J mol ⁻¹ K ⁻¹]
T	Temperature [K]
a	PR and PSRK coefficients [bar m ² mol ⁻²]
b	PR and PSRK coefficients [m ³ mol ⁻¹]

LIST OF FIGURES

Figure 1: Flare gas undergoing combustion (Elvidge et al. 2016).	1
Figure 2: Membrane-based separation (Khanipour et al., 2017).	9
Figure 3: Integrated gasification and dry reforming process in parallel (adapted from Alibrahim et al., 2021).	11
Figure 4: Integrated gasification and dry reforming process in series (adapted from Alibrahim et al., 2021).	11
Figure 5: A typical steam reformer design (Tran et al., 2017).	14
Figure 6: Global production of methanol by the year 2014 (adapted from Galadima and Muraza, 2015).	17
Figure 7: Parity plot for the fractional conversion of CO (adapted from Bussche and Froment, 1996).	21
Figure 8: Parity plot for the fractional CO ₂ conversion (adapted from Bussche and Froment, 1996).	21
Figure 9: Methanol production using Lurgi's technology (Rahmatmand et al., 2019)...	22
Figure 10: Syngas production PFD	31
Figure 11: Methanol production PFD.....	34
Figure 12: Comparison of the simulation results with those documented by Borreguero et al. (2020).	36
Figure 13: Effect of temperature on the equilibrium TRM reactor product.	38
Figure 14: Effect of the H ₂ O/CH ₄ ratio in the TRM reactor and pressure on the quality of the produced syngas.	40
Figure 15: Effect of the pressure on the output of the MeOH reactor.	41
Figure 16: Effect of the pressure on the amount of methanol vented.	42
Figure 17: Effect of the temperature on the produced methanol.	43
Figure 18: Effect of the syngas H ₂ /CO ratio on the produced methanol.	44
Figure 19: Plant energy consumption for heating and cooling process streams.	45
Figure 20: Actual and planned heating utilities for the Plant.	46
Figure 21: Actual and planned cooling utilities for the Plant.	46
Figure 22: Plant HEN diagram.	48
Figure 23: Amount of energy saved after the designed HEN.	50
Figure 24: World average inflation rates of product prices.	54
Figure 25: Accumulated cash flow over different years.	56
Figure 26: CO ₂ equivalent emissions reduction with and no project implemented.	56

LIST OF TABLES

Table 1: Kinetic expressions and parameters used in the TRM reactor (Borreguero et al., 2020).....	16
Table 2: Constants used kinetic model (Graaf et al., 1988).	20
Table 3: Constants of the kinetic model (Bussche and Froment, 1996).....	20
Table 4: Reactor, catalyst and feed stream features for methanol production (Nestler et al., 2020; Rahmatmand et al., 2019).....	23
Table 5: Raw materials used for the syngas production.....	28
Table 6: Main simulation results for syngas production	32
Table 7: Overall simulation results in the methanol production section.	35
Table 8: Comparison of the main methanol production properties, current simulation results and those from Luyben (2010).....	37
Table 9: Heat exchangers features from the designed HEN.....	49
Table 10: Process and utility streams features from the designed HEN.	50
Table 11: Acquisition costs for the main equipment.....	52
Table 12: Results of the percentage method for fixed capital investment.....	53

CHAPTER I

INTRODUCTION

1.1 Background

In recent decades, the Earth has faced significant environmental challenges, mainly related to CO₂ emissions released into the atmosphere as a result of human activities such as the combustion of fossil fuels for energy and transport, deforestation and industrial processes. These emissions contribute significantly to climate change and global warming, and part of these emissions are associated with gas flaring (Bergougui, 2024; Khanipour et al., 2020; Stančín et al., 2020).

Gas flaring is a commonly utilized method for the disposal of natural gas generated at oil and gas facilities where the existing infrastructure is insufficient to capture the entire gas output, as illustrated in Figure 1 and emphasized in Elvidge et al. (2016). This practice not only leads to greenhouse gas emissions into the atmosphere but also results in economic losses as valuable hydrocarbon resources are wasted.

Figure 1 illustrates quantities of radiant energy that are produced by gas flares where their statistics are accessed by data taken directly from a satellite launched in 2012 under the monitoring of the United States National Oceanic and Atmospheric Administration (NOAA).



Figure 1: Flare gas undergoing combustion (Elvidge et al. 2016).

The Global Gas Flaring Reduction Partnership (GGFR) by the World Bank collaborates with governments, oil companies, and international organizations to formulate policies and regulations aimed at achieving zero routine flaring up to 2030, as outlined by (Dinani et al., 2023a).

Based on this data, the worldwide gas flaring amounted to 150 billion m³ in 2019, indicating a 3% rise from 2018 and matching the total annual gas consumption of Sub-Saharan Africa. It is worth mentioning that natural gas operations have promising potential to reduce greenhouse gas emissions and improve the utilization of flare gas, as outlined in Al-Khori et al. (2021).

An excellent method for enhancing and making use of flare gas involves integrating it into methanol production, as suggested by Khalili-Garakani et al. (2022) and Khanipour et al. (2020). In this process, flare gas is blended with the incoming natural gas feed and then transformed into syngas.

For large-scale syngas production, the predominant industrial technology involves the Steam Reforming of Methane (SRM) process, which uses Nickel-based catalysts supported on alumina (Ni/Al₂O₃), taking place at temperatures ranging from 700 to 900 °C and at low pressures, in which CH₄ reacts with steam to produce gaseous mixture of H₂ and CO. There are other technologies for producing syngas, such as Dry Reforming of Methane (DRM) and Partial Oxidation of Methane (POM).

A noteworthy technology, known as Tri-reforming of Methane (TRM), is attracting widespread interest globally for syngas production from natural gas. This innovative approach results from combining the three technologies already mentioned (SRM, DRM, and POM) and is appreciated for its benefits in both technical and environmental aspects.

The syngas generated is introduced into a multi-tubular reactor, where the reactors are commonly packed with a copper-based catalyst supported by alumina (Cu/ZnO/Al₂O₃) for methanol production. This process occurs within a temperature range of 200 to 300 °C and pressures between 50 and 100 bar. The reaction is mildly exothermic, necessitating a cooling system to remove the produced heat and maintain a constant temperature inside the reactor. For this purpose, a cooling gas or boiling water is used (Rahmatmand et al., 2019).

This research will primarily focus on incorporating flare gas into methanol production, optimizing heat requirements and energy efficiency in syngas production through the tri-reforming process and subsequent methanol production, and examining the influence of thermodynamic parameters on both processes.

1.2 Motivation

Mozambique possesses extensive natural gas reserves, with one of the largest reserves situated in the Mozambique Basin, Inhambane province, specifically in the Pande/Temane fields. The extraction and production activities in these fields have been undertaken by Sasol Petroleum Temane since 2004, commencing with a contracted capacity of 120 MGJ/a and an initial investment totaling 1.2 billion US\$.

By 2009, Sasol expanded production capacity from 120 to 183 MGJ/a; at present, the company's production stands at approximately 190 MGJ/a. About 80% of this gas is exported to South Africa, while the remaining portion is sold on the domestic market.

The recent discovery of additional natural gas reserves along the Inhassoro coast in the southern region of Mozambique by Sasol Petroleum Temane suggests the increase of local use of natural gas, beyond primarily piping it to South Africa. To cope with the abundance of natural gas targeted for local use, additional ways of utilizing natural gas are needed.

One promising strategy involves establishing facilities to expand natural gas value chain, such as the construction of a methanol production Plant. This initiative holds the potential to stimulate the country's economic growth and simultaneously address unemployment by providing opportunities for young people, who will contribute as labour to the Plant.

The produced methanol can serve as a feedstock for dimethyl ether production, which has the potential to replace diesel fuel due to its high cetane number (greater than 55), low atmospheric pollutants emission, efficient combustion, and reduced smoke formation. Using dimethyl ether as a diesel substitute could significantly reduce the funds spent on fuel imports, as diesel is currently the most imported fuel in Mozambique.

The expected results of this research could be important for Empresa Nacional de Hidrocarbonetos (ENH), which has every interest in creating all the necessary conditions for the construction and operation of a methanol production Plant.

1.3 Research problem

Currently, the majority of natural gas processing Plants opt to flare the excess gas into the atmosphere. This choice results from the impracticality of economically storing gas quantities that surpass the needed capacity for customs supply and internal Plant usage. Unfortunately, gas-flaring process contributes to greenhouse gas emissions and results in the inefficient dissipation of energy.

In chasing of the Paris Agreement's goal of reducing greenhouse gas emissions by around 50% by 2030, and in line with the trend towards energy transition, there is growing consideration for more sustainable technologies. Integrating flare gas into methanol production process has emerged as one of the potential answers to these challenges. Although this approach offers an appealing solution for minimizing greenhouse gas emissions, there are several challenges associated with its practical implementation.

A significant challenge in integrating flue gas into methanol production lies in the catalyst deactivation that occurs during the DRM and SRM reactions throughout syngas production. Addressing this challenge involves potential enhancements to both the catalytic and feed aspects of the process. Regarding the TRM reactor feed, it is essential to maintain an excess of steam over it.

In terms of catalysis, the critical factor is the development of catalysts that are not only more active but also more stable. Traditional catalysts, particularly Nickel-based ones, commonly face deactivation issues due to carbon deposition and sintering at high temperatures, as highlighted by Fedorova et al. (2020). While advanced catalysts with improved resistance to deactivation and higher reaction rates could enhance overall process performance. However, they are not the primary focus of this research.

Another obstacle to incorporating flare gas into methanol production based on tri-reforming technology in the production of syngas is the substantial endothermic nature of the SRM and DRM processes. This characteristic demands a significant amount of heat input to drive the reactions forward, posing technical and economic difficulties. A solution to this challenge involves leveraging waste heat from the process.

By harnessing excess heat from hot sources, such as the product stream or fired heater flue gas, the energy demand of SRM and DRM can be partially satisfied, leading to an overall reduction in energy consumption. Moreover, optimizing the process and

employing heat recovery techniques can enhance the energy efficiency of tri-reforming technology.

Advanced heat exchangers and strategic process design can effectively capture and utilize waste heat generated throughout the methanol production process, thereby minimizing the reliance on external energy input.

1.4. Research limitations

This study is based on theoretical research, utilizing available data and referencing notable work in the corresponding field. It began with an extensive literature review on syngas production, emphasizing the catalysts, kinetics and thermodynamics relevant to the subsequent production of methanol.

Aspen HYSYS was chosen for the syngas production simulation because it is a widely used tool in the industry for modeling chemical processes, ranging from individual unit operations to entire chemical Plants and refineries.

Aspen HYSYS can handle essential chemical engineering calculations, including mass and energy balances, vapor-liquid equilibrium, heat and mass transfer, chemical kinetics, fractionation, and pressure drops, as well as it performs calculations based solely on reactor volume, which is advantageous because most proposed kinetic models for syngas production are designed based on the reactor volume.

The main limitation found in the use of Aspen HYSYS is in its inability to simulate chemical processes that require the use of more than one thermodynamic package in the same flowsheet. This problem arises in this study, where more than one thermodynamic package is used, namely the PR equation of state for the syngas production simulation and the PSRK equation of state for the methanol production simulation.

Another limitation when using Aspen HYSYS is that it cannot perform calculations based on the catalyst weight during simulation. This is problematic because the proposed kinetic models for methanol production are developed based on catalyst weight. This issue was resolved by using Aspen PLUS simulator (which shares many similarities with Aspen HYSYS) for the methanol production section simulation. Aspen PLUS allows calculations based on catalyst weight and supports the PSRK equation of state.

The main focus of the research centered on simulation. It did not extend to carrying out practical experiments to check whether the theoretical results obtained from the simulation are in line with observations in practice.

1.5 Research objectives

1.5.1 General objective

The general objective of this research is to evaluate the techno-economic feasibility of incorporating flare gas into the tri-reforming process of methanol production.

1.5.2 Specific objectives

The specific objectives of this research are:

- To evaluate the overall conversion of CH₄ present in natural gas and flare gas into syngas that is suitable for methanol production;
- To evaluate the overall conversion of CO, CO₂, and H₂ present in the produced syngas into methanol;
- To determine the properties of the methanol produced;
- To investigate the impact of key operating conditions (temperature, pressure, and feed composition) on the reaction rates of syngas and methanol production processes;
- To determine the optimal operating conditions for the syngas and methanol production processes.
- To assess the potential energy savings through heat integration approach.
- To estimate the Net Present Value (NPV) and Internal Rate of Return (IRR) of the project.

CHAPTER II

LITERATURE VIEW

2.1 Introduction

This chapter reviews the existing body of research on methanol production, with specific emphasis on catalyst development, reaction mechanisms, process optimization and potential applications. Through an assessment of the progress and challenges in this field, the review aims to offer a perspective on the feasibility of integrating flare gas into methanol production, taking into account the evolution of the energy landscape and climate-related concerns.

Methanol production through the conversion of syngas derived from natural gas is a well-established industrial process. The upcoming sections will primarily concentrate on the production of syngas via tri-reforming of methane process. A concise overview of the technologies employed will be provided, along with a contextualization and justification of the chosen technologies in the context of this research.

2.2 Flare gas

Many gas and oil-producing nations frequently waste valuable hydrocarbon gases, which possess a high heating value. Instead of being utilized, these gases are often flared or vented. Consequently, these countries suffer substantial losses in terms of both energy and economic resources, as explained by Tahouni et al. (2016). According to Anomohanran (2012) and Asadi et al. (2021), gas flaring not only results in the wastage of a potentially valuable energy source but also contributes significantly to carbon emissions into the atmosphere.

Discharging natural gas through flaring or venting directly into the atmosphere is identified as a fundamental contributor to greenhouse gases emissions (Heidari et al. 2016). Roughly, 5% of the global natural gas supply is lost due to flaring and/or venting, resulting in the release of approximately 300 million tons of CO₂ annually into the environment (Ojijiagwo et al., 2016). This considerable volume of flared gas holds the potential for practical applications, such as methanol production, as discussed in Soltanieh et al. (2016) and Khanipour et al. (2020).

Besides methanol production, several alternative approaches for reclaiming flare gas include: (i) injecting flare gas into gas reservoirs for capture and sequestration, (ii) employing compression techniques for gas storage, (iii) utilizing it as feedstock for

petrochemical processes, (iv) generating electricity using gas turbines, and (v) producing fuels such as petrol, kerosene, Liquefied Petroleum Gas (LPG), and diesel through Fischer-Tropsch technology (Dinani et al., 2023 and Hamidzadeh et al., 2020).

The effective operation and reliability of various equipment used in a gas processing Plant, such as flash drums for separating liquid and gas, pneumatic valves for gas circulation in different units, reboilers for heating up mixtures to enhance separation based on density and boiling point differences, and heat exchangers, are highly dependent on pressure control. Conversely, a sudden increase in pressure in these devices could potentially damage them or compromise their integrity. Hence, it is essential to maintain precise pressure control.

Pressure control is maintained through the installation of Pressure Safety Valves (PSV) and blowdown valves right after the gas outlet of the protected equipment. These valves in normal operating conditions are closed and when the gas pressure within a particular equipment, such as a flash drum, exceeds its designated pressure set point, they open, allowing the gas to be vented to the flare system for combustion. The gas that is vented and then flared is known as *flare gas* and has a high CH₄ content and may contain other valuable hydrocarbons.

While the process of flaring the excess gas released in that protected equipment ensures safety, it results in the loss of valuable gas resources. In order to recover the valuable chemical components within the flare gas stream, an efficient and feasible separation method must be implemented. Cryogenic distillation and Pressure Swing Adsorption (PSA) processes are viable options, although they are associated with elevated operating costs and substantial energy requirements.

This challenge can be addressed by employing membrane-based separation, as illustrated in Figure 2; it offers advantages such as low energy consumption, cost-effectiveness, operational feasibility, compactness, and safety. Different membranes have been employed for the purification of flare gas and consist of polyimide-based membranes such as Matrimid 5218, a Palladium/Silver alloy membrane, and a co-polyimide hollow fiber membrane named P84, as discussed in Khanipour et al. (2017).

Figure 2 shows four steps in the membrane-based separation process used to separate components such as H₂ in order to increase the yields of syngas production for subsequent methanol production.

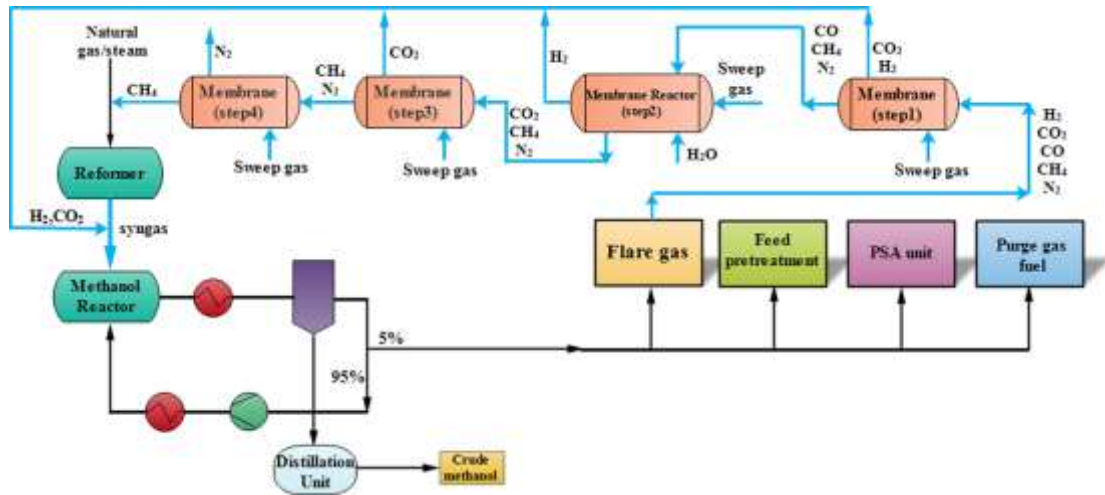


Figure 2: Membrane-based separation (Khanipour et al., 2017).

In step 1, a membrane is used to separate CO_2 and H_2 from the flare gas, which consists of N_2 , CH_4 , CO , CO_2 , and H_2 . In step 2, CO is converted into H_2 and CO_2 via the Water Gas Shift (WGS) reaction, facilitated by the presence of steam. The resulting H_2 is then separated using a membrane. In step 3, CO_2 is extracted with another membrane, and in step 4, N_2 is removed through a membrane as well.

After step 4, the remaining flare gas, mainly composed of CH_4 , is blended with a natural gas stream. This mixture is sent to a reformer to produce syngas, which is then combined with H_2 and CO_2 and fed into a reactor to produce methanol.

2.3 Syngas production process

Syngas, also known as synthesis gas, is a mixture of H_2 and CO , containing traces of chemical compounds such as CO_2 and CH_4 . It serves as the crucial basis for Hydrogen production and plays a key role as feedstock for petrochemical industry. The global annual revenue generated from syngas is approximately 6 Exajoules (EJ), being employed in activities related to petroleum refining, ammonia fertilizer production, and methanol manufacturing (Chafik, 2021; Farniaei et al., 2014).

In 2019, around 75% of the worldwide syngas production was used as raw material for the manufacture of chemicals products, 22% was transformed into both gaseous and liquid fuels, while the remaining 3% of syngas was employed for power generation according to Alibrahim et al. (2021).

Various technologies for producing syngas are well documented, depending on factors such as the input material, oxidizing agent, desired syngas composition, and the intended

use downstream. Nevertheless, gasification of solid materials such as coal and biomass as well as the reforming of methane are the most prevalent technologies within the commonly utilized commercial methods for syngas production according to Alibrahim et al. (2021).

Fazlikeshteli et al. (2024) and Hasanat et al. (2023) state that the fundamental reactions involved in the production of syngas through methane conversion include: (i) Dry Reforming of Methane (DRM) described by equation (2.1); (ii) Partial Oxidation of Methane (POM) denoted by equation (2.2); and (iii) the Steam Reforming of Methane (SRM) represented by equation (2.3).



DRM is a process where CO_2 reacts with CH_4 , converting these compounds with considerable global warming potential into valuable chemicals. DRM process typically has elevated operating temperatures, reaching up to 800°C , utilizing reforming catalysts such as Nickel-based catalyst.

One problem encountered in DRM is the formation of carbon, resulting in catalyst deactivation due to the highly endothermic nature of the process. The syngas generated from DRM has a lower H_2/CO ratio, which is of 1 as evidenced by equation (2.1), making it not suitable for methanol production. A H_2/CO ratio between 1.5 and 3 is deemed optimal for the methanol production (Song and Pan, 2004 and Khajeh et al., 2014).

Significantly, the substantial energy requirements for endothermic DRM procedures can be provided and maintained using renewable energy sources like Concentrating Solar Power (CSP). This approach proves to be viable for North African countries, as indicated by an economic and carbon footprint assessment study (Chafik, 2021).

The technology of DRM, utilized in syngas production, is environmentally beneficial as it mitigates the release of CO_2 into the atmosphere, addressing concerns related to global warming and climate change. However, its economic feasibility is hindered by the substantial energy requirements. To address this challenge, technology enhancement involves combining DRM technology, known for its high-energy demand, with gasification technology, recognized for its high-energy release. To achieve this,

Alibrahim et al. (2021) suggest two distinct configurations: one in parallel and the other in series.

Figure 3 and Figure 4, show parallel and series configuration loops, respectively; both figures illustrate the energy derived from the gasification process, which is then utilized to support the DRM process, ultimately contributing to sustainable syngas production. The energy efficiency of the DRM process is approximately 73%, whereas when combined with a gasification process, the efficiency increases to around 84% (Alibrahim et al., 2021).

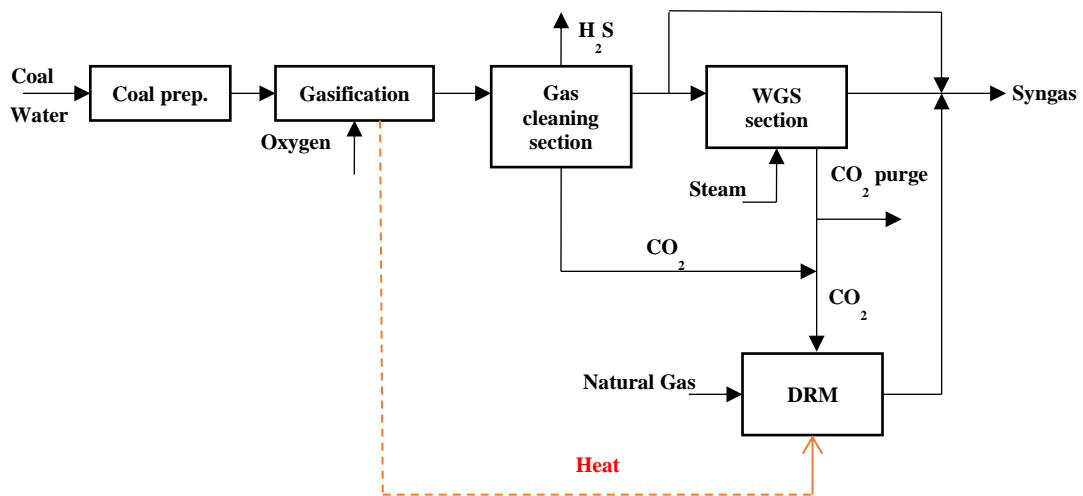


Figure 3: Integrated gasification and dry reforming process in parallel (adapted from Alibrahim et al., 2021).

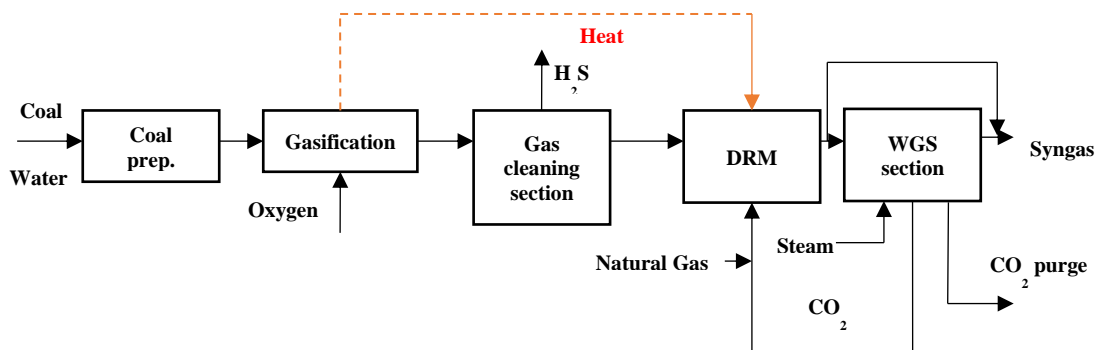
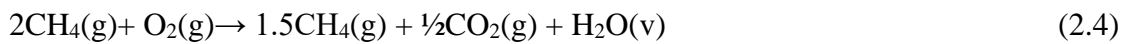


Figure 4: Integrated gasification and dry reforming process in series (adapted from Alibrahim et al., 2021).

Partial Oxidation of Methane (POM) has the capability to generate syngas through two distinct reaction pathways. The direct reaction pathway is a single-step process where syngas is directly produced from methane, as illustrated in equation (2.2).

On the other hand, the indirect reaction pathway involves the initial conversion of CH₄ to steam and CO₂ described by equation (2.4) and subsequent transformation into syngas through reforming equations (2.1) and (2.3), as indicated in Hasanat et al. (2023). POM itself can be performed without the need for an external heat source since it is mildly exothermic process, as highlighted in Fazlikeshteli et al. (2024).



The POM process is advantageous as it achieves high CH₄ conversion rate and favorable selectivity in a short residence time; furthermore, the POM produces an excellent H₂/CO ratio of 2, making it suitable for Fischer-Tropsch synthesis as well as methanol production. Nevertheless, the exothermic nature of this reaction is a crucial factor, leading to the development of hotspots that could potentially damage the reactor and raise safety concerns.

Additionally, achieving CH₄ conversion to syngas at high temperatures in the absence of a catalyst is a requirement, prompting the exploration of various catalyst systems for POM, as discussed in Hasanat et al. (2023).

Steam Reforming of Methane (SRM) is the predominant method for the large-scale generation of hydrogen-rich syngas. In this procedure, CH₄ and steam undergo a reaction facilitated by a catalyst, resulting in the production of hydrogen-rich syngas. Due to the highly endothermic nature of the reaction, elevated temperatures are essential to achieve significant conversion levels (Carapellucci and Giordano, 2020).

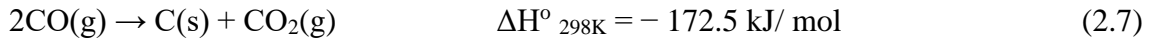
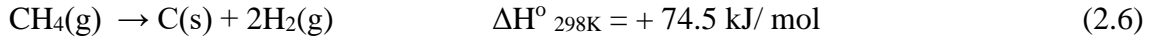
The primary governing reactions in this process are the thermodynamically independent steam methane reforming reaction given by the reaction equation (2.3) and Water Gas Shift (WGS) reaction denoted by reaction equation (2.5), as outlined in From et al. (2024).



The WGS reaction is initiated to decrease the molar fraction of CO and enhance the rate of H₂ production (Carapellucci and Giordano, 2020). Given the strong endothermic nature of the SRM process, high-operating temperatures in the range of 700 to 900 °C are required to achieve consistent conversion of CH₄ into H₂. Additionally, following the Le

Chatelier's principle, low pressures are conducive to promoting SRM since the reaction involves an increase in the number of molecules.

Besides the high-energy demand in SRM process, another issue faced is the formation of coke, a result of CH₄ decomposition and the Boudouard reaction given by equations (2.6) and (2.7), respectively. This can lead to catalyst deactivation due to carbon deposition.



To prevent the deactivation of the catalyst, SRM is commonly conducted with an intentional surplus of steam (Carapellucci and Giordano, 2020). Another cause of catalyst deactivation is the presence of higher hydrocarbons in the natural gas feed during syngas production, which can convert to olefins through steam cracking. These olefins can eventually form coke in the SRM reactor. This issue can be mitigated by oxidizing the higher hydrocarbons before they enter the SRM reactor.

The traditional SRM reactor adopts a design comprising a furnace with a shell and tube configuration. The core of the process unfolds within a specific number of reforming tubes made of high alloy, each filled with a catalyst. Typically, Nickel serves as the catalyst material due to its ability to strike a balance between thermo-chemical performance and cost-effectiveness.

Alumina (Al₂O₃) particles support the catalyst, and their size and shape are carefully tailored to maximize the surface-to-volume ratio while minimizing pressure drops inside the tubes. The thermal power required for the endothermic reaction is supplied by the reformer shell-side, achieved through either burning additional fuel or potentially harnessing the waste heat from gas turbines (Carapellucci and Giordano, 2020).

Usually, the fired reformer stands out as the most substantial, intricate, and costly unit operation within the syngas production process. It comprises a multitude of high-alloy steel tubes filled with catalyst material, arranged in a large furnace. This furnace is heated through the combustion of fossil fuels and off-gases produced in the process. In this arrangement, approximately half of the provided heat is directly conveyed to the reforming reaction within the catalyst bed, with the remainder exiting as latent heat carried by the hot flue gas, which exceeds 1000 °C (From et al., 2024).

Figure 5 illustrates the isometric view of an industrial-scale, top-fired, co-current reformer with 336 reforming tubes, which are symbolized by 336 smaller circles, 96 burners, which are denoted by 96 larger circles, and 8 flue gas tunnels, which are represented by 8 rectangular intrusions.

Steam Reforming of Methane (SRM) technology generates syngas with a H_2/CO molar ratio of 3, see equation (2.3). This pathway is extensively employed in various industries for syngas production (Osman et al., 2021). Since this molar ratio is favorable for methanol production, the SRM technology could be used exclusively in this research. However, the research will not be based solely on SRM technology due to its high-energy requirements and high CO_2 emissions (Katebah et al., 2022).

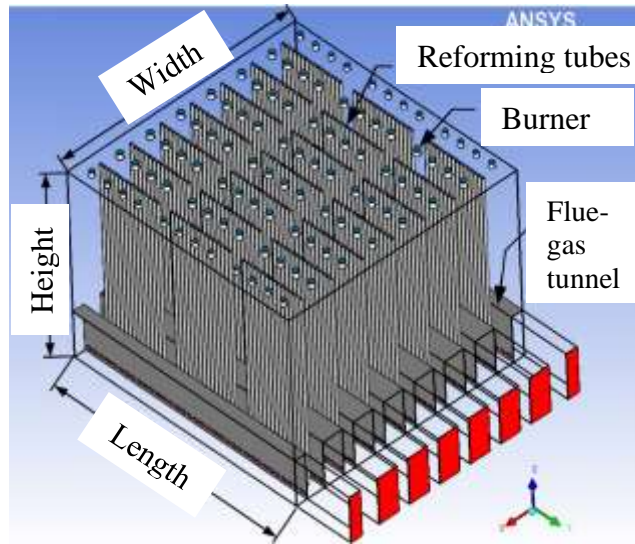


Figure 5: A typical steam reformer design (Tran et al., 2017).

To address the challenges associated with SRM technology, the tri-reforming of methane process was suggested. This approach combines DRM, POM, and SRM technologies (Manenti et al., 2015; Osat and Shojaati, 2022). This hybrid approach offers several advantages such as the flexibility of adjusting the H_2/CO molar ratio by controlling the proportions of each co-reactant.

Additionally, it boasts lower energy consumption compared to SRM, thanks to the inclusion of exothermic reactions occurring during POM. Moreover, the catalyst stability is enhanced as it mitigates coke formation, attributed to the presence of strong oxidants such as H_2O and O_2 (Borreguero et al., 2020; Osat and Shojaati, 2022). Therefore, in this research, the tri-reforming of methane process has been selected for the production of syngas.

Due to their cost-effectiveness, widespread accessibility, and high reactivity, catalysts based on Nickel have been widely employed in reforming processes. The characteristics and composition of catalysts play a crucial role in the conversion of CO₂ in the tri-reforming process, especially in the temperature range of 700 to 850 °C at 1 atm. In the tri-reforming experiments, the catalysts exhibited varying capacities to improve CO₂ conversion, following the sequence Ni/MgO > Ni/MgO/CeZrO > Ni/CeO₂ > Ni/Al₂O₃ > Ni/CeZrO.

Song and Pan (2004) believe that the CO₂ conversion observed with Ni/MgO and Ni/MgO/CeZrO in tri-reforming is attributed to the interaction between CO₂ and MgO, along with a greater interface between Ni and MgO facilitated by the creation of a NiO/MgO solid solution.

The prevalent and widely utilized reactor for the tri-reforming process is a fixed-bed reactor. Nonetheless, a fluidized-bed tri-reformer reactor is proposed as a promising alternative for syngas production due to its favorable temperature profile, primarily attributed to its effective heat management. This arrangement offers several advantages over a fixed-bed reactor, such as increased CH₄ conversion (1.2%), greater CO₂ consumption (6%), and energy savings (Tomishige, 2004 and Khajeh et al., 2014).

Additionally, the temperature of the hot spot in the catalytic bed decreases from 1407 °C to 1159 °C. Consequently, the fluidized-bed tri-reformer reactor surpasses the fixed-bed configuration and is regarded as a promising setup for syngas production (Khajeh et al., 2014).

The kinetic model for the tri-reforming of methane process widely employed in both fixed-bed and fluidized-bed reactors, relies on the mathematical equations presented in Table 1.

It is assumed that POM approaches full conversion when oxygen is virtually undetectable in the effluent gas. These equations are outlined in Borreguero et al. (2020) and derived from the mechanism proposed by Wei and Iglesia (2004) for steam and dry reforming reactions, while the kinetic equation for the WGS reaction is adopted from the work by De La Osa et al. (2011).

Table 1: Kinetic expressions and parameters used in the TRM reactor (Borreguero et al., 2020).

Reaction	Kinetic expressions	Parameters
SRM	$r_{SRM} = k_1' P_{CH_4} \left(1 - \frac{P_{CO} P_{H_2}^3}{P_{CH_4} P_{CO_2} K_{SRM}} \right)$	$k_1^0 = 85.77 \text{ mol.s}^{-1} \cdot \text{kPa}^{-1}$
	$K_{SRM} = 1.198E17 \cdot e^{\left(\frac{-26830}{T}\right)}$	$E_{a1} = 74.72 \text{ kJ mol}^{-1}$
	$k_1' = k_1^0 \cdot e^{\left(\frac{-E_{a1}}{RT}\right)}$	
DRM	$r_{DRM} = k_2' P_{CH_4} \left(1 - \frac{P_{CO}^2 P_{H_2}^2}{P_{CH_4} P_{CO_2} K_{DRM}} \right)$	$k_2^0 = 70.99 \text{ mol.s}^{-1} \cdot \text{kPa}^{-1}$
	$K_{DRM} = 6.78E18 \cdot e^{\left(\frac{-31230}{T}\right)}$	$E_{a2} = 77.82 \text{ kJ mol}^{-1}$
	$k_2' = k_2^0 \cdot e^{\left(\frac{-E_{a2}}{RT}\right)}$	
WGS	$r_{WGS} = k_3' \left(\frac{P_{CO} P_{H_2O}}{P_{H_2}} - \frac{P_{CO_2}}{k_{eqWGS}} \right)$	$k_3^0 = 149.92 \text{ mol.s}^{-1} \cdot \text{kPa}^{-1}$
	$k_{eqWGS} = 10^{\left(\frac{2073}{T} - 2,2029\right)}$	$E_{a3} = 54.26 \text{ kJ mol}^{-1}$
	$k_3' = k_3^0 \cdot e^{\left(\frac{-E_{a3}}{RT}\right)}$	

2.4 Overview of the methanol production process

Methanol has a great relevance in the energy sector; it is an important chemical product that can be used directly as a fuel or mixed with petrol due its properties as well as serving as an intermediate molecule for various chemical syntheses, such as olefins, amines, acetic acid, dimethyl ether and formaldehyde, as highlighted in Ribeiro Domingos et al. (2022), in Santos et al. (2018), as well as in Sehested (2019).

Methanol is one of the most important basic chemical products worldwide having an annual production close to 112 million tons and its production began in 1923, when Baden Aniline and Soda Factory (BASF) introduced the first commercial thermochemical methanol production process which involves the hydrogenation of CO to methanol on a ZnO-Cr₂O₃ catalyst at temperatures ranging from 350 to 400 °C and pressures of 240 to 300 bar (Nestler et al., 2020; Rahmatmand et al., 2019).

In 1966, Imperial Chemical Industries (ICI) secured a patent for the initial commercially implemented low-pressure synthesis process, allowing for pressures below 150 bar and

temperatures below 300 °C through the utilization of a Cu-Zn based catalyst. While this catalytic system is predominantly utilized in industrial processes to this day, both catalyst manufacturers and scientists consistently report on improvements related to activity and catalyst lifespan (Fan et al., 2017).

Methanol production technologies of nowadays involve two key catalytic processes: the generation of syngas, followed by the conversion of the produced syngas into methanol. The primary raw materials used for syngas production include natural gas, methane gas from associated petroleum, shale gas, coal, and biomass as highlighted in Galadima and Muraza (2015) and Nestler et al. (2020).

Figure 6 provides a visual representation of the global methanol production in 2014, constituting 80% of the current output, with China emerging as the primary producer.

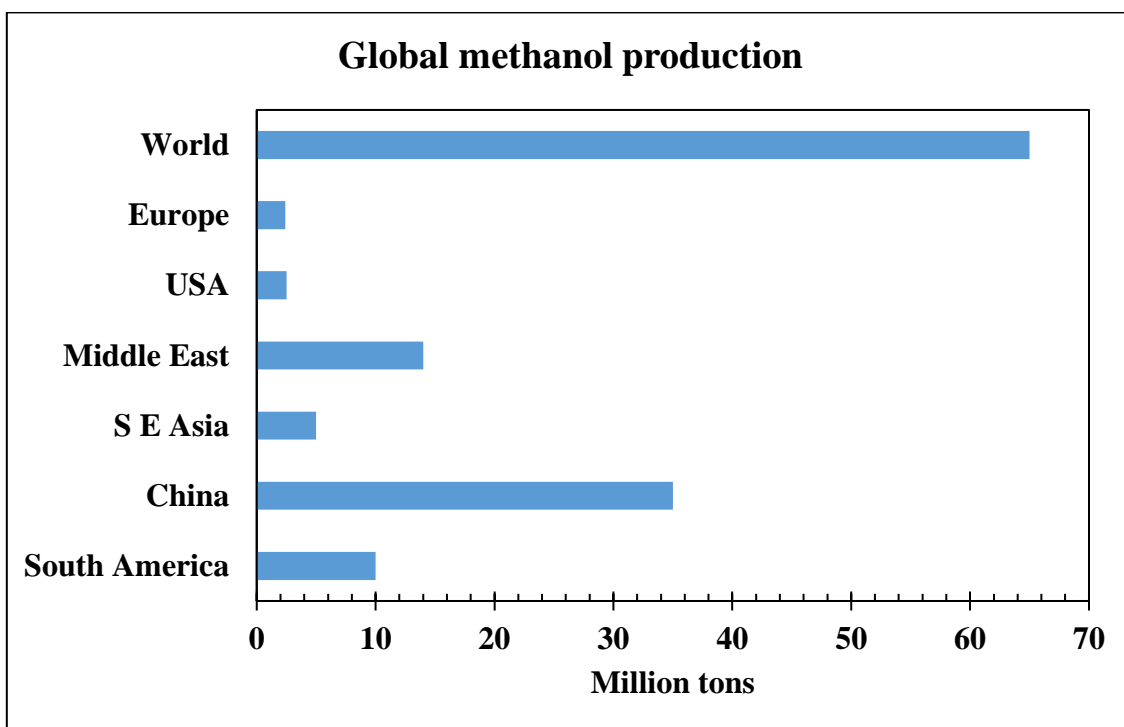


Figure 6: Global production of methanol by the year 2014 (adapted from Galadima and Muraza, 2015).

Methanol production process is currently performed by employing a Cu/ZnO/Al₂O₃ catalyst, operating at temperatures spanning from 200 to 300 °C and pressures ranging between 50 and 100 bar. The methanol production reaction is constrained by chemical equilibrium, with higher methanol yields achieved at lower temperatures and higher

pressures. Consequently, the recycling of unreacted gas becomes imperative to attain elevated conversions (Ribeiro Domingos et al., 2022).

2.4.1 Reaction schemes

The process of methanol production is controlled by a mechanism involving the Reverse Water Gas Shift (RWGS) reaction given by equation (2.8). In this reaction, CO₂ undergoes a transformation into CO and H₂O. Additionally, the mechanism includes the hydrogenation conversion of both CO and CO₂ into methanol, as outlined in reactions (2.9) and (2.10), respectively (Ay et al., 2021; Rahmatmand et al., 2019).



The sum of equations (2.8) and (2.9) result in the following reaction process:



2.4.2 Kinetic modelling

Graaf et al. (1988) introduced a kinetic rate model featuring three reaction rate equations expressed through equations (2.11) to (2.13) corresponding the equations (2.8), (2.9) and (2.10). In doing so, the authors did not take into account that certain intermediates are involved in hydrogenation and RWGS reactions.

$$r_1 = \frac{k_1 K_{CO} \left[f_{CO} f_{H_2}^{3/2} - \frac{f_{CH_3OH}}{f_{H_2}^{1/2} K_{p1}} \right]}{\left(1 + K_{CO} f_{CO} + K_{CO_2} f_{CO_2} \right) \left[f_{H_2}^{1/2} + \left(\frac{K_{H_2O}}{K_{H_2}^{1/2}} \right) f_{H_2O} \right]} \quad (2.11)$$

$$r_2 = \frac{k_2 K_{CO_2} \left[f_{CO_2} f_{H_2} - \frac{f_{H_2} f_{CO}}{K_{p2}} \right]}{\left(1 + K_{CO} f_{CO} + K_{CO_2} f_{CO_2} \right) \left[f_{H_2}^{1/2} + \left(\frac{K_{H_2O}}{K_{H_2}^{1/2}} \right) f_{H_2O} \right]} \quad (2.12)$$

$$r_3 = \frac{k_3 K_{CO_2} \left[f_{CO_2} f_{H_2}^{3/2} - \frac{f_{CH_3OH} f_{H_2O}}{f_{H_2}^{1/2} K_{p3}} \right]}{\left(1 + K_{CO} f_{CO} + K_{CO_2} f_{CO_2} \right) \left[f_{H_2}^{1/2} + \left(\frac{K_{H_2O}}{K_{H_2}^{1/2}} \right) f_{H_2O} \right]} \quad (2.13)$$

Consequently, the model simultaneously predicts two different concentrations of the same intermediate. To address this challenge, Bussche and Froment (1996) proposed a mechanistic model assuming that CO₂ is the main source of carbon in methanol production; this assumption accounts for only two reaction rate equations indicated by equations (2.14) and (2.15) which correspond to the equations (2.8) and (2.10).

$$r_1 = k_1 P_{CO_2} P_{H_2} \frac{\left(1 - \frac{P_{H_2O} P_{CH_3OH}}{K_{E1} P_{H_2}^3 P_{CO_2}} \right)}{\left(1 + k_2 \frac{P_{H_2O}}{P_{H_2}} + k_3 P_{H_2}^{1/2} + k_4 P_{H_2O} \right)^3} \quad (2.14)$$

$$r_2 = k_5 P_{CO_2} \frac{\left(1 - \frac{P_{H_2O} P_{CO}}{K_{E2} P_{H_2} P_{CO_2}} \right)}{\left(1 + k_2 \frac{P_{H_2O}}{P_{H_2}} + k_3 P_{H_2}^{1/2} + k_4 P_{H_2O} \right)} \quad (2.15)$$

The reaction rates r_1 and r_2 are given in [mol/kg_{cat}.s] and the partial pressures P_{H_2O} , P_{CH_3OH} , P_{CO_2} and P_{H_2} in [bar].

The rate constants proposed by Graaf et al. (1988) are presented in Table 2 and those suggested by Bussche and Froment (1996) are presented in Table 3.

Table 2: Constants used kinetic model (Graaf et al., 1988).

Constants of adsorption equilibrium		
$K = A \exp\left(\frac{B}{TR}\right)$	A	B
K_{CO_2}	$(7.050 \pm 1.390) \cdot 10^{-7}$	61700 ± 800
$\frac{K_{H_2O}}{K_{H_2}^{1/2}}$	$(6.370 \pm 2.880) \cdot 10^{-9}$	84000 ± 1400
K_{CO}	$(2.160 \pm 0.440) \cdot 10^{-5}$	46800 ± 800
Constants of equilibrium		
$k_p = 10^{\left(\frac{A}{T-B}\right)}$	A	B
k_{p1}	5139	12.621
k_{p2}	3066	10.592
k_{p3}	- 2073	- 2.029
Constants of rate		
$k = A \exp\left(\frac{B}{RT}\right)$	A	B
k_1	$(4.890 \pm 0.029) \cdot 10^7$	- 63000 \pm 300
k_2	$(9.640 \pm 7.300) \cdot 10^{11}$	- 152900 \pm 6800
k_3	$(1.090 \pm 0.070) \cdot 10^5$	- 87500 \pm 300

Table 3: Constants of the kinetic model (Bussche and Froment, 1996).

Constant	Value
K_{E1}	$10^{\left(\frac{3066}{T} - 10.592\right)}$
K_{E2}	$10^{\left(-\frac{2073}{T} + 2.029\right)}$
k_1	$1.07 \text{EXP}\left(\frac{36696}{RT}\right)$
k_2	3453.38
k_3	$0.499 \text{EXP}\left(\frac{17197}{RT}\right)$
k_4	$6.62 \cdot 10^{-11} \text{EXP}\left(\frac{124119}{RT}\right)$
k_5	$1.22 \cdot 10^{10} \text{EXP}\left(-\frac{94765}{RT}\right)$

Figures 7 and 8 illustrate the excellent agreement between the calculated and experimental conversions of CO and CO₂, respectively. This shows the reliability of the kinetic model proposed by Bussche and Froment (1996).

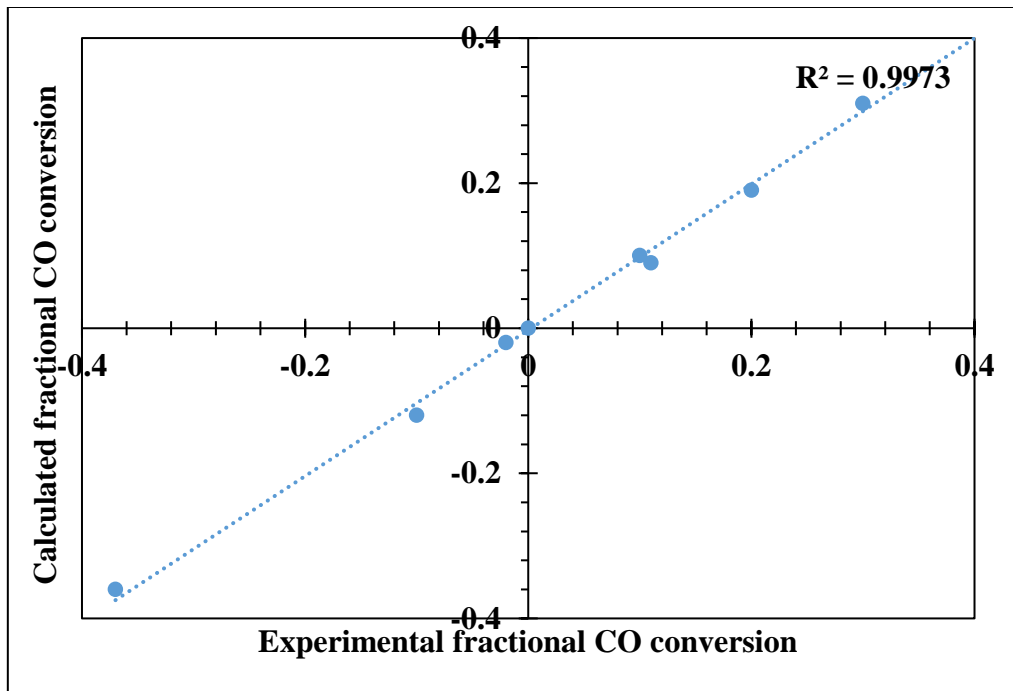


Figure 7: Parity plot for the fractional conversion of CO (adapted from Bussche and Froment, 1996).

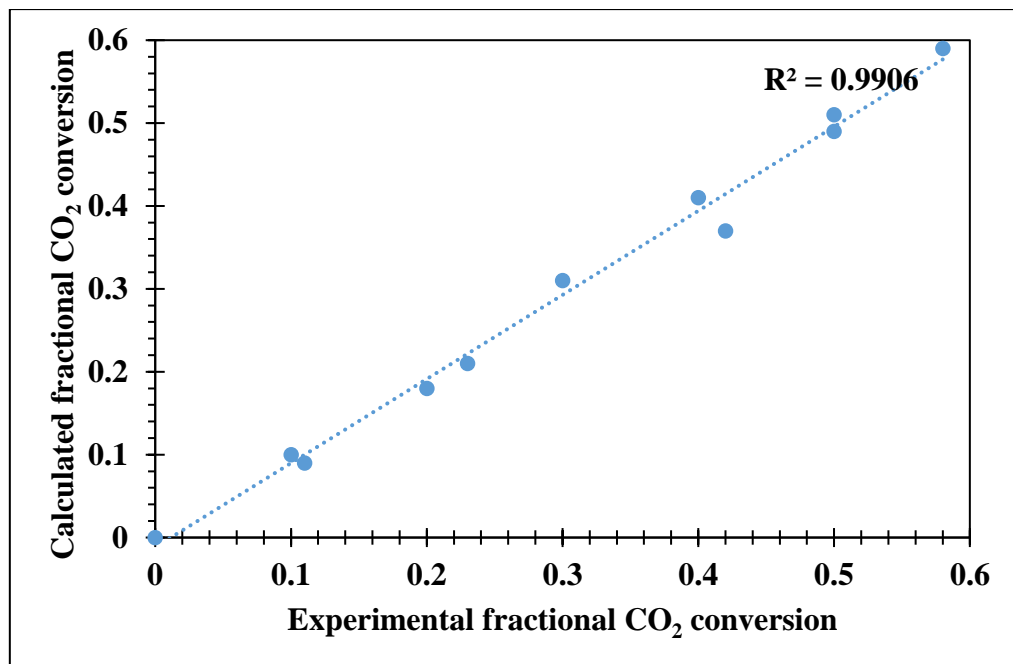


Figure 8: Parity plot for the fractional CO₂ conversion (adapted from Bussche and Froment, 1996).

2.5 Reactor for methanol production

Various reactor configurations are available, with fixed-bed reactors featuring a cooling system being the primary choices for industrial applications. These reactors are typically filled with a Copper-based catalyst supported by alumina ($\text{Cu}/\text{ZnO}/\text{Al}_2\text{O}_3$). Among these configurations, the Lurgi externally-cooled, multi-tubular catalytic technology stands out as the most widely utilized commercially (Ribeiro Domingos et al., 2022 and Rahmatmand et al., 2019).

When aiming for significant methanol production capacities up to 3000 t/d, the use of a single reactor, in the process as described by Luyben (2010), is considered unsuitable. As a solution, Lurgi's technology is adopted, which employs two-stage converter system combining two Lurgi methanol reactors (Rahmatmand et al., 2019). The configuration utilized in Lurgi's technology for methanol production is depicted in Figure 9.

In this technology, the initial phase of methanol production takes place in a water-cooled reactor. The reactions take place in tubes with a $\text{Cu}/\text{ZnO}/\text{Al}_2\text{O}_3$ catalyst, while water circulates through the casing to extract heat from the reaction side. The temperature on the cooling side of the water-cooled reactor remains constant. Subsequently, the product from the first reactor (stream VII) enters the shell of the gas-cooled reactor, constituting the second phase of methanol production.

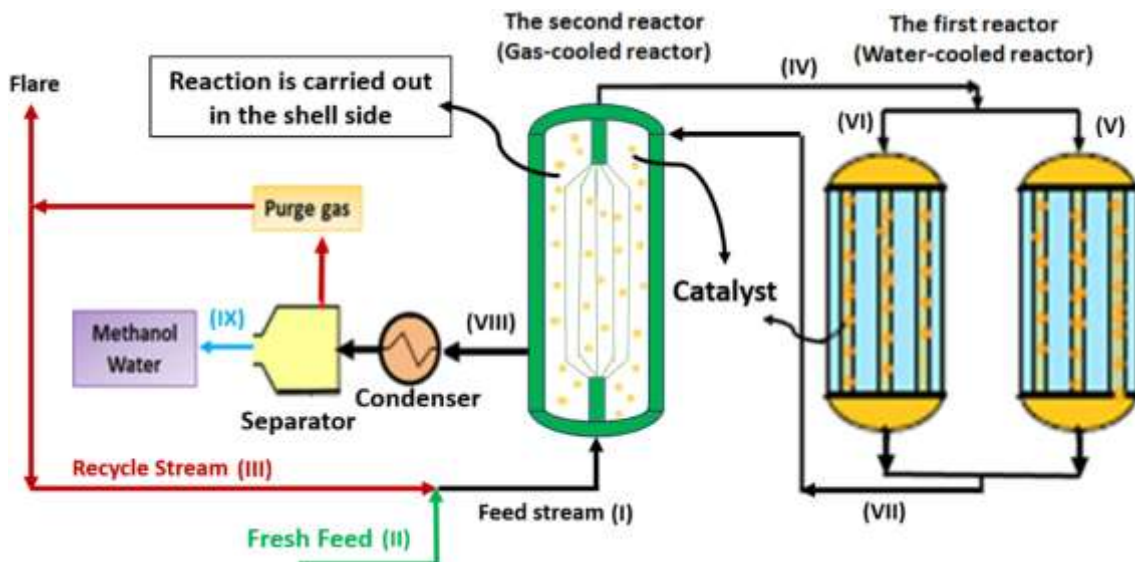


Figure 9: Methanol production using Lurgi's technology (Rahmatmand et al., 2019).

The chemical reactions depicted by equations (2.9) and (2.10); release heat and result in a reduction in the number of moles. This shows the need for operating at high pressure

and low temperature to favor the equilibrium towards methanol production. Consequently, methanol reactors are maintained within a temperature range of 220 to 250 °C and a pressure of 50 bar (Osman et al., 2021 and Luyben, 2010).

To achieve nearly isothermal operation and, consequently, enhance per-pass conversion to methanol, the reactors undergo continuous cooling through the circulation of a cooling gas or a boiling water stream at a pressure ranging between 40 and 50 bar on the shell side. The reactor and catalyst parameters commonly used industrially for methanol production are presented in Table 4.

Table 4: Reactor, catalyst and feed stream features for methanol production (Nestler et al., 2020; Rahmatmand et al., 2019).

Parameter	Suggested value	Range
Catalyst density (kg/m ³)	1775	N/A
Particle diameter (m)	0.004	0.004 – 0.008
Bed voidage	0.5	0.4 – 0.6
Tube length (m)	8	6 – 12
Tube diameter (m)	0.05	0.04 – 0.12
Number of tubes	5000	2000 – 10000
Reactor diameter (m)	Adjustable	N/A
Inlet feed temperature (°C)	200	180 – 250
Maximum reactor peak temperature (°C)	280	N/A

Mitsubishi Gas Chemical (MGC) and Mitsubishi Heavy Industry (MHI) developed an isothermal reactor known as the MGC/MHI superconverter. This reactor features double-walled tubes with the catalyst loaded in the space between the outer and inner tubes, as described by Tijm et al. (2001). The syngas is introduced at the bottom of the vessel through flexible tubes and flows upward inside the inner shell of these tubes.

Upon reaching the top, the syngas turns downward and passes into the annular space where the catalyst is situated. Cooling water flows outside the tubes. The mixture of methanol and unreacted syngas exits from the bottom of the vessel.

Another example of a fixed bed reactor used in methanol production is the Linde isothermal reactor. It contains helically coiled tubes within the catalyst bed, enabling

indirect heat exchange. This reactor configuration is also ideal for exothermic catalytic reactions. The cooling tubes ensure the highest possible reaction rate and an optimal temperature profile (Bozzano and Manenti, 2016).

CHAPTER III

RESEARCH MATERIALS, METHODS AND STRATEGIES

3.1 Introduction

This chapter provides a thorough overview of the research methodologies and techniques utilized to address the research problem and accomplish the objectives of this research. It covers the fundamental aspects of kinetics, property predictions, research tools, and methods, as well as the key parameters considered for methanol production.

Most of previous studies, simulated chemical reactions processes based on stoichiometry or equilibrium models. The equilibrium model approach, despite its simplicity, the obtained results are quite limited and do not offer comprehensive insights into the process characteristics. To address this limitation, there is a need for more studies to simulate the reactions processes using kinetic-based models. These would be beneficial for reactor sizing, sensitivity analysis, cost calculation as well as instrumentation and control.

3.2 Tools for Plant simulation and economic analysis

In this research, the methanol production through syngas will be simulated using the Aspen Tech Simulation Softwares (Aspen HYSYS and Aspen PLUS). The simulation model will incorporate mass balance, energy balance, and momentum balance, utilizing the software's embedded equations and incorporating kinetic expressions in Plug Flow Reactors (PFR).

In this work, Peng-Robinson (PR) equation of state was selected as the thermodynamic package to estimate fluid properties for the syngas production simulation. This choice is based on the versatility of the PR model to handling a broad range of temperatures and pressures, along with the availability of extensive binary interaction parameters for fugacity calculation. The PR equation of state is well-suited for dealing with chemical reactions involving mixtures of hydrocarbons, steam, O₂, and combustion gases. The PR equation of state is given by equation (2.16).

$$p = \frac{RT}{v-b} - \frac{a(T)}{v(v+b)+b(v-b)} \quad (2.16)$$

Where the parameters “a” and “b” are obtained at a critical point:

$$a = 0.45724 \frac{R^2 T_c^2}{P_c} \quad (2.17)$$

$$b = 0.07780 \frac{RT_c}{P_c} \quad (2.18)$$

For a given set of temperature and pressure conditions for methanol production, and the presence of polar components (methanol and water), the Predictive Soave–Redlich–Kwong (PSRK) equation of state has been selected to simulate the methanol production section. The PSRK model is given by equation (2.19), its parameters are determined through the equations (2.20) to (2.23).

$$P = \frac{RT}{v-b} - \frac{a\alpha(T)}{v(v+b)} \quad (2.19)$$

In the PSRK equation, the α -function is given as

$$\alpha(T_r) = \left[1 + c_1 \left(1 - T_r^{1/2} \right) \right]^2 \quad (2.20)$$

The parameter c_1 can be obtained from the acentric factor, ω , using the relation

$$c_1 = 0,48 + 1,574\omega - 0,176\omega^2 \quad (2.21)$$

The PSRK mixing rule calculates the parameters a and b of the equation of state by

$$\frac{a}{bRT} = \sum_i x_i \frac{a_i}{b_i RT} - \frac{\frac{g_o^E}{RT} + \sum x_i \ln \frac{b}{b_i}}{0,64663} \quad (2.22)$$

and

$$b = \sum_i x_i b_i \quad (2.23)$$

where the parameters a_i and b_i correspond to the pure substances, with their mole fractions represented by x_i , and the excess Gibbs energy represented by g_o^E . The excess Gibbs energy is determined using a modified version of the UNIFAC model.

PSRK model calculates activity coefficients based on the functional groups within the molecules that compose the liquid mixture. By considering the interactions of each functional group and some binary interaction coefficients, the activity of each solution can be determined. This data is essential for understanding liquid equilibria, which is crucial for various thermodynamic calculations, including chemical reactor design and distillation processes.

A Plug Flow Reactor (PFR) is a simplified one-dimensional reactor model in which, at each point-along the reactor, the velocity of the reactive phase (e.g. concentrations, and temperature and pressure) remains constant along the cross-section. There is no back-mixing in the PFR, and it features a single inlet and outlet. Before operating the PFR, information about the reactions is necessary.

For the PFR applied to simulate a chemical process in a given simulator, a reaction package must be assigned so that reactions can be specified accordingly. Kinetic reactions rate, can be defined as homogeneous or heterogeneous. In the case of heterogeneous reactions, it is essential to provide details about catalyst properties (Guamán-Marquines et al., 2023 and Luyben, 2010).

In the work, the economic viability of incorporating flare gas into methanol production process is assessed through Aspen Process Economic Analyzer (APEA) package. It adopts a specialized approach tailored to the standardized economic evaluation of novel chemical and energy Plants, as proposed by Pruvost et al. (2022).

To optimize the energy needed for cooling and heating the process streams during syngas and methanol production, heat integration is achieved by implementing a Heat Exchanger Network (HEN) using the Aspen Energy Analyzer (AEA) tool.

For data analysis and graph plotting, Microsoft Excel was selected because it offers essential spreadsheet features, organizing data in a grid of cells arranged in numbered rows and letter-named columns. It supports various data manipulations, including arithmetic operations, and provides a range of functions for statistical and engineering goals.

3.3 Materials

In order to get success and great results when simulating a chemical process Plant is required to well define the input data by specifying all the conditions introduced in the simulator. In this work the composition in mole fraction of the raw materials for the syngas production which include Low Pressure Flare Gas (LPFG), High Pressure Flare Gas, Natural Gas (NG), water and oxygen used in the pre-reactors are presented in Table 5. The mass flow employed for LPFG, HPFG, NG, Water, O₂_1, O₂_2 and O₂_3 are 2513 kg/h, 488 kg/h, 37050 kg/h, 52390 kg/h, 11200 kg/h and 192 kg/h respectively. All of them are in 25 °C and 1 atm.

Table 5: Raw materials used for the syngas production

Variable	LPFG	HPFG	NG	Water	O _{2_1}	O _{2_2}	O _{2_3}
CH ₄	0.7801	0.8592	0.9433	0	0	0	0
C ₂ H ₆	0.0332	0.0223	0.0209	0	0	0	0
C ₃ H ₈	0.0240	0.0131	0.0081	0	0	0	0
i-C ₄ H ₁₀	0.0064	0.0028	0.0021	0	0	0	0
n-C ₄ H ₁₀	0.0076	0.0032	0.0025	0	0	0	0
i-C ₅ H ₁₂	0.0029	0.0011	0.0008	0	0	0	0
n-C ₅ H ₁₂	0.0028	0.0010	0.0005	0	0	0	0
C ₆ H ₁₄	0.0021	0.0004	0.0002	0	0	0	0
C ₇ H ₁₆	0.0028	0.0002	0.0001	0	0	0	0
C ₈ H ₁₈	0.0012	0.0001	0	0	0	0	0
C ₉ H ₂₀	0.009	0	0	0	0	0	0
CO	0	0	0	0	0	0	0
CO ₂	0.0037	0.0002	0	0	0	0	0
H ₂	0	0	0	0	0	0	0
CH ₃ OH	0	0	0	0	0	0	0
O ₂	0	0	0	0	1	1	1
H ₂ O	0	0	0	1	0	0	0
N ₂	0.1334	0.0963	0.0215	0	0	0	0

3.4 Key parameters for methanol production process simulation

The characteristics of the reactors employed in methanol production must be carefully determined and defined based on the desired yields. Given that chemical reactions are involved in the process, it is crucial to thoroughly consider the nature of the reaction, whether it is exothermic or endothermic. This consideration helps determine the most suitable approach to achieve high yields of the desired product.

In the case of exothermic reactions, it is not recommended to operate at high temperatures, since they release heat and therefore are preferable at low temperatures, as is the case with the hydrogenation of CO₂ producing methanol and water, as described in equation (2.10). In addition, pressure is another physical parameter that, if not properly determined, reduces yields based on the Le Chatelier's principle.

Selecting an optimal range of operating temperature and pressure is synonymous with determining the operating conditions, a critical factor in the simulation of the methanol production process. Other key parameters directly associated with reactor design include: physical dimensions, reaction kinetics, feed conditions and thermodynamic package.

CHAPTER IV

RESULTS AND DISCUSSION

4.1 Introduction

The purpose of this chapter is to present the key results of the simulation for syngas production and further methanol production. This include parameters such as reaction temperature, pressure, and feed composition in both the Tri-reforming of Methane (TRM) reactor and the methanol (MeOH) reactor that affect the effectiveness of syngas production and methanol production through sensitivity analysis. Additionally, it aims to provide an economic assessment of the project implementation to determine its economic feasibility and to quantify the energy savings achieved through the implementation of Heat Exchanger Network (HEN).

Since the results presented in this chapter are based solely on simulations using the tools discussed in the previous chapter, the validation of these simulations results is done by comparing them with data reported in the open literature.

4.2 Syngas production results

Figure 10 shows the Aspen HYSYS simulated-based layout of natural gas reforming industrial Plant for the production of syngas. The layout incorporates four reactors identified as "Pre-reactor_1," "Pre-reactor_2," "Pre-reactor_3," and "TRM reactor." The Pre-reactors were utilized to guarantee the conversion of heavier hydrocarbons found in the Natural Gas (NG), Low Pressure Flare Gas (LPFG), and High Pressure Flare Gas (HPFG) streams in the presence of O₂, preventing them from reaching the TRM reactor.

This measure aimed to avoid potential catalyst deactivation in the syngas production process due to carbon deposition caused by heavier hydrocarbons. The Pre-reactors were also utilized to generate heat, which is used in the Steam Reforming of Methane (SRM) and Dry Reforming of Methane (DRM) reactions. This approach helps prevent excessively high temperatures, as observed by Kim et al. (2010), Borreguero et al. (2020) and Zhang et al. (2013), where a furnace is used to produce heat for SRM and DRM reactions through methane combustion, resulting in temperatures exceeding 3000 °C.

To ensure that all the heavier hydrocarbons react and generate heat, the pre-reactors were supplied with precisely calculated amount of oxygen (O₂). The amount of O₂ were determined using Gibbs reactors, considering the thermodynamic properties of the reactions (operating pressure, temperature, and natural gas feed quantity).

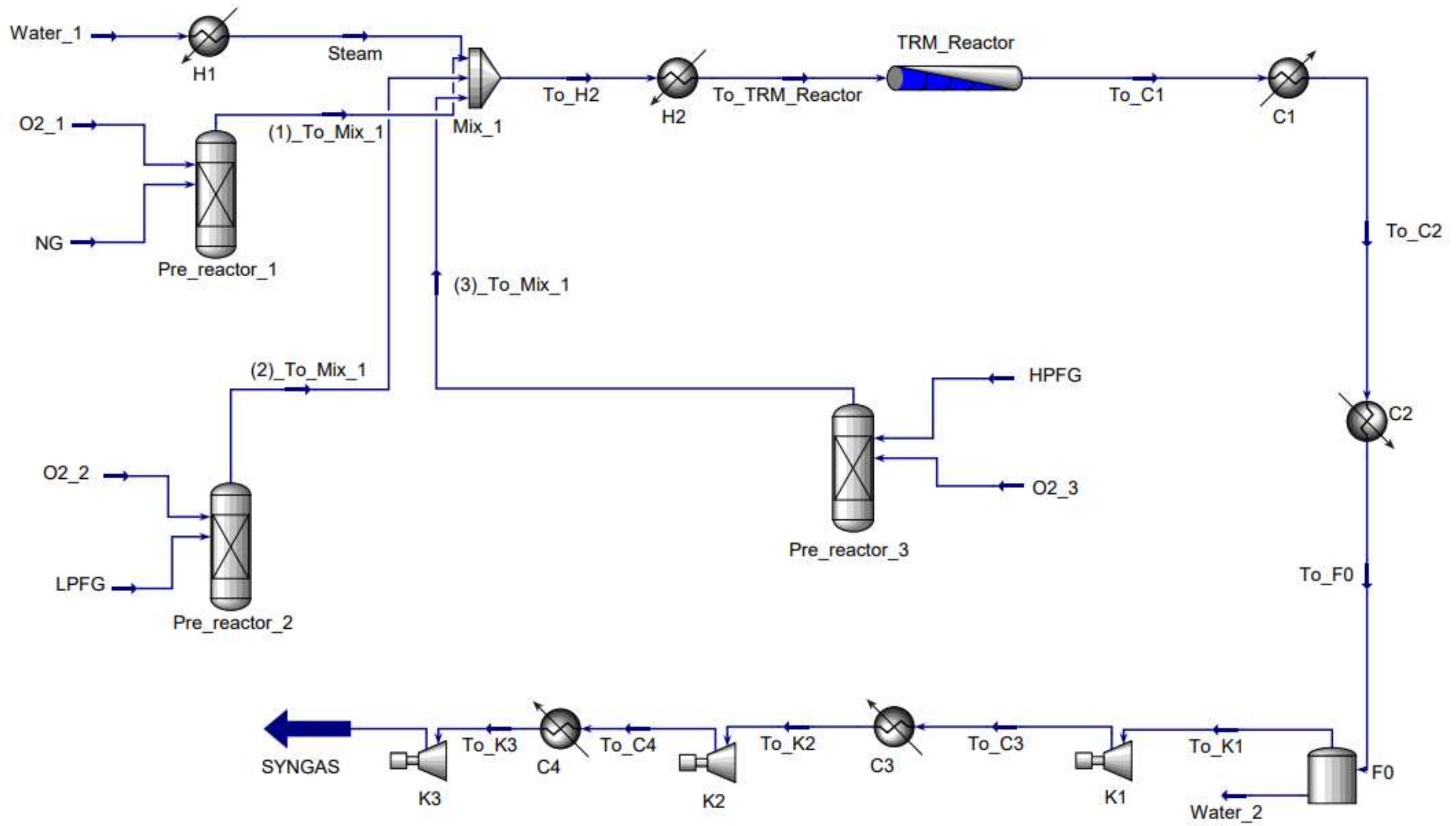


Figure 10: Syngas production PFD

The calculated ratios of O₂ to feed are 0.1617 for "Pre-reactor_1," 0.3781 for "Pre-reactor_2," and 0.2251 for "Pre-reactor_3." The effluents from "Pre-reactor_1," "Pre-reactor_2," and "Pre-reactor_3," named as "(1)_To_Mix_1", "(2)_To_Mix_1", "(3)_To_Mix_1" and having temperatures of 999 °C, 1665 °C, and 1270 °C, respectively, are combined with vaporized water at 100 °C in the unit called "Mix_1." The resulting mixture, with a temperature of 710 °C, is then heated to 850 °C. This was carried out to optimize the rates of the SRM and DRM reactions occurring in the TRM reactor. The composition of the produced SYNGAS is given in Table 6.

Table 6: Main simulation results for syngas production

Variable	LPFG	HPFG	NG	To_TRM	SYNGAS
Mass flow (kg/h)	2513	487.9	37050	105350	88370
Temperature (°C)	25	25	25	850	220
Pressure (atm)	1	1	1	1	50
CH ₄ (mole fraction)	0.7801	0.8592	0.9433	0.3784	0.0042
C ₂ H ₆ (mole fraction)	0.0332	0.0223	0.0209	0	0
C ₃ H ₈ (mole fraction)	0.0240	0.0131	0.0081	0	0
i-C ₄ H ₁₀ (mole fraction)	0.0064	0.0028	0.0021	0	0
n-C ₄ H ₁₀ (mole fraction)	0.0076	0.0032	0.0025	0	0
i-C ₅ H ₁₂ (mole fraction)	0.0029	0.0011	0.0008	0	0
n-C ₅ H ₁₂ (mole fraction)	0.0028	0.0010	0.0005	0	0
C ₆ H ₁₄ (mole fraction)	0.0021	0.0004	0.0002	0	0
C ₇ H ₁₆ (mole fraction)	0.0028	0.0002	0.0001	0	0
C ₈ H ₁₈ (mole fraction)	0.0012	0.0001	0	0	0
C ₉ H ₂₀ (mole fraction)	0.009	0	0	0	0
CO (mole fraction)	0	0	0	0	0.2474
CO ₂ (mole fraction)	0.0037	0.0002	0	0.0419	0.0149
H ₂ (mole fraction)	0	0	0	0	0.6953
CH ₃ OH (mole fraction)	0	0	0	0	0
H ₂ O (mole fraction)	0	0	0	0.5678	0.0309
N ₂ (mole fraction)	0.1334	0.0963	0.0215	0.0119	0.0073
H ₂ /CO molar ratio	N/A	N/A	N/A	N/A	2.81

The product from the TRM reactor undergoes cooling through two coolers to reach ambient temperature (25 °C) before being directed to the flash drum labeled as "F0" to eliminate liquid-phase water via the stream named "Water_2." The vapor outlet from the flash drum is subjected to compression through three compressors until reaching 50 atm.

As gas compression induces temperature elevation, two coolers are integrated in between the compressors. The output stream from the compressor "K3" is referred to as "SYNGAS" and will serve as the input stream for the methanol production section.

4.3 Methanol production results

As mentioned above, the production of methanol was carried out employing Aspen PLUS simulator. For this purpose, the SYNGAS obtained from Aspen HYSYS with composition provided in Table 5 constituted the main input data.

Figure 11 presents the simulation-based methanol production Process Flow Diagram (PFD). Fresh syngas feed at 50 atm and 220 °C is blended in the mixture labeled as "M1" with the vapor gases stream labeled "15" exiting the flash drum denoted as "F3" and the stream "12". Stream "12" is formed by combining the vapor gases stream "8" from the flash drum labeled "F1" with the vapor gases stream "9" from the flash drum labeled "F2."

Prior to their integration into the respective mixtures, streams "9," "8," and "15" undergo compression up to 50 atm. The resulting stream "0", mixture "M1" exits at a pressure of 50 atm and a temperature of 71 °C. It is then heated to 220°C to align with the operational requirements of the MeOH reactor.

The MeOH reactor operates adiabatically, indicating that there is no heat exchange through the reactor walls. As a result, the internal temperatures of the reactor rise significantly since the methanol production reaction is inherently exothermic. Without proper temperature control within the reactor, there's a risk of damaging the reactor and lowering the conversion rates of the reactants, ultimately impacting the yields of the desired product.

To avoid temperature rises inside the reactor and maintain stability, a stream of thermal fluid at 217 °C is used, which flows through tubes connected to the MeOH reactor and has an overall heat transfer of 1021 kJ/hm²C.

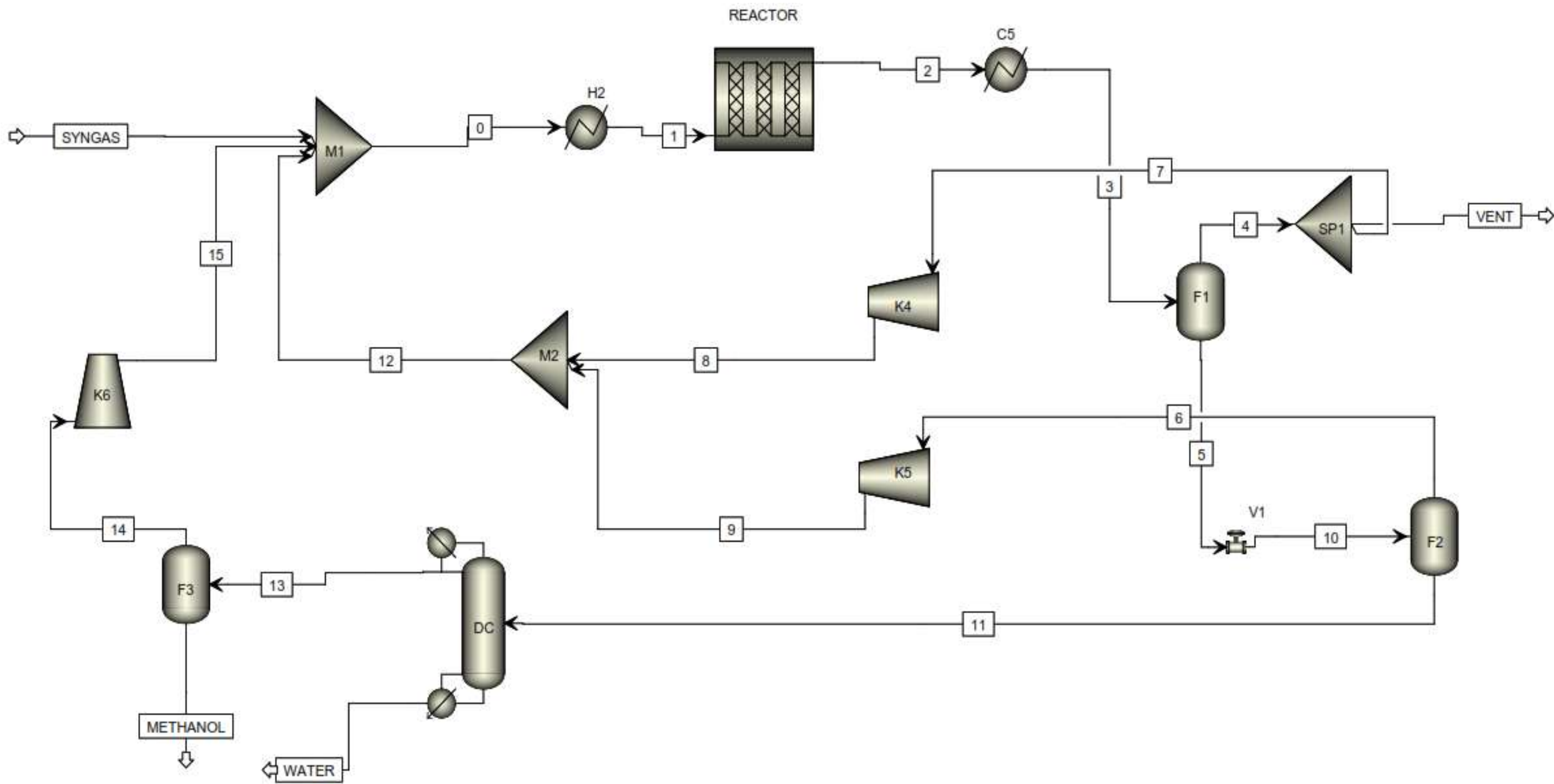


Figure 11: Methanol production PFD

The product from the MeOH reactor is cooled by 50 °C to facilitate the condensation of CH₃OH and H₂O before being directed to the flash drum labeled "F1" to segregate liquids from the gas. Subsequently, 98% of the gas stream exiting the flash drum "F1" is recycled back to the MeOH reactor, while the remaining portion is vented.

The liquid stream exiting the flash drum "F1" at approximately 50 atm pressure is depressurized to 2 atm and directed to the flash drum "F2" to eliminate the lighter components present in the gas stream produced during the flash drum operation. The pressure reduction is performed to enhance the separation between the liquid and gas phases.

The resulting gas stream from flash drum "F2" is recycled back to the MeOH reactor, while the liquid stream is transferred to the distillation unit, operating at 1 atm pressure with a reflux ratio of 0.407 and equipped with 42 stages. The column feed is introduced at stage 27.

The liquid stream at the bottom of the column contains water with 100% purity. The stream above the column flows into flash drum "F3" to separate light components from the methanol, which has a purity of 98% mole fraction. The light components are returned to the MeOH reactor. Table 7 provides overall results in the methanol production section.

Table 7: Overall simulation results in the methanol production section.

Variable	Stream "1"	Stream "5"	Stream "11"	METHANOL
Mass flow (kg/h)	385848	82108	81649	75433
Temperature (°C)	220	50	44	45
Pressure (atm)	50	50	2	1
CH ₄ (mole fraction)	0.023258	0.000781	0.000066	0.000043
N ₂ (mole fraction)	0.040314	0.000485	0.000014	0.000005
CO ₂ (mole fraction)	0.008165	0.001164	0.000429	0.000440
H ₂ O (mole fraction)	0.004385	0.146935	0.148916	0.026233
H ₂ (mole fraction)	0.876391	0.009769	0.000282	0.000094
CO (mole fraction)	0.037080	0.000121	0.000004	0.000002
CH ₃ OH (mole fraction)	0.010408	0.840745	0.850289	0.983184

4.4 Validation of the simulation process

The simulation results obtained in this work, which are based on mathematical kinetic equations in the TRM reactor, were validated by comparing them with those documented by Borreguero et al. (2020) for a similar process. The key process streams in the tri-reforming section pertain primarily to the TRM reactor, where the reactants CH_4 and CO_2 undergo SRM and DRM, respectively, to produce syngas.

Furthermore, the crucial factor in the TRM reactor is the H_2/CO ratio in the syngas flow, as it directly influences methanol production rates, i.e. high methanol production rates are obtained when there are high H_2/CO molar ratios.

Figure 12 compares the results obtained from the simulation performed in this research with those from Borreguero et al. (2020). It compares the composition of the input and output streams of the TRM reactor, as well as the H_2/CO ratio in the syngas flow under various $\text{H}_2\text{O}/\text{CH}_4$ ratios in the reactor feed. These comparisons were conducted at a temperature of $850\text{ }^\circ\text{C}$ and a pressure of 1 atm.

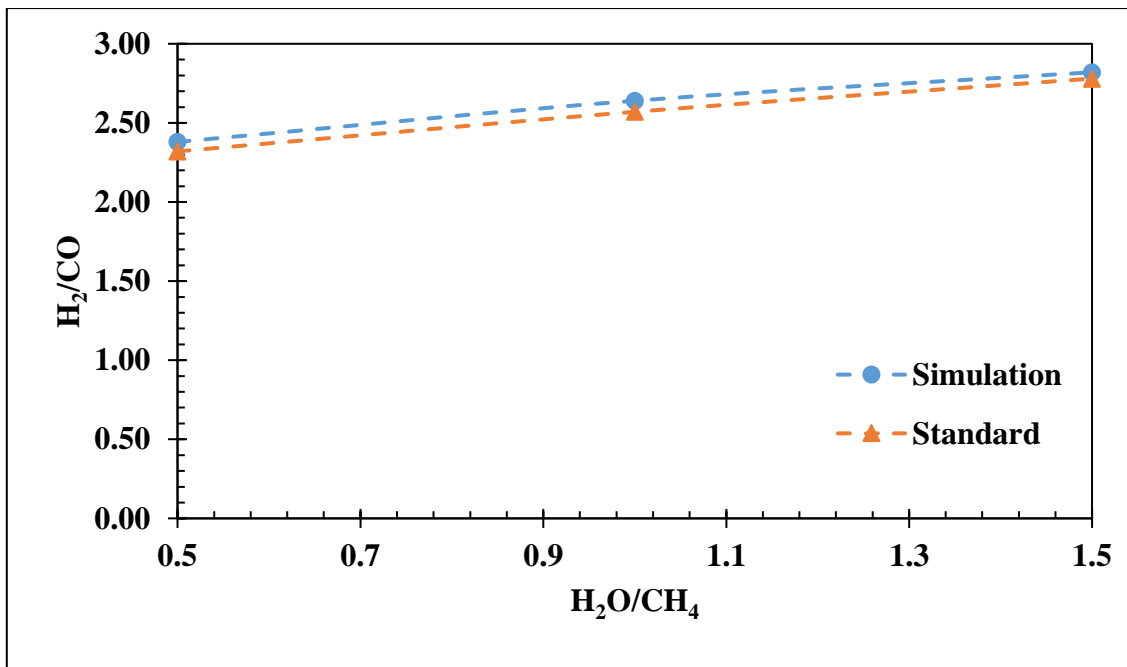


Figure 12: Comparison of the simulation results with those documented by Borreguero et al. (2020).

The simulated H_2/CO ratio in the syngas stream differs from the value computed by Borreguero et al. (2020) by approximately 2.6% when the $\text{H}_2\text{O}/\text{CH}_4$ ratio in the TRM

reactor is 0.5. This deviation slightly increases to 2.7% when the H₂O/CH₄ ratio is set to 1, and decreases to 1.4% when a ratio of 1.5 is applied.

The suitability of using the developed model, which is based on mathematical kinetic equations in the TRM reactor, to simulate the tri-reforming process is therefore demonstrated, once the deviations are below 5%. The values derived from Borreguero et al. (2020) are regarded as the standard as they represent the actual operating conditions for a typical tri-reforming process in the Industry.

The validation of the methanol production simulation was conducted by comparing the outcomes with those documented by Luyben (2010). Identical operating parameters of the reactor (150 °C and 110 bar) were applied for this comparison. The evaluated factors include the conversion rates of the carbon source reactants for methanol production and the quality of the resulting methanol and water in terms of purity. These comparisons, along with their respective deviation magnitudes, are presented in Table 8.

Table 8: Comparison of the main methanol production properties, current simulation results and those from Luyben (2010).

Property	Simulation	Luyben	Deviation
CO conversion	0.997	0.987	1.0%
CO ₂ conversion	0.976	0.911	7.1%
Overall CO and CO ₂ conversion	0.996	0.960	3.7%
H ₂ O purity	1.000	1.000	0.0%
CH ₃ OH purity	0.980	0.990	1.0%

The deviation between the CO₂ conversion value obtained in this work and that reported by Luyben (2010) is approximately 7.1%. This discrepancy can be attributed to the composition of the syngas used in this work, which contains less CO₂ compared to the syngas used by Luyben (2010). Consequently, the current simulation results in higher consumption of CO₂ due to the abundance of H₂ available for reaction, leading to elevated conversion rates. If Luyben (2010) had employed syngas with a lower CO₂ content, the CO₂ conversion rate would likely have been higher, exceeding 91.1% and aligning more closely with the results of the developed simulation.

The CO conversion, H₂O purity, CH₃OH purity, and the overall CO and CO₂ conversion exhibit deviations of 1%, 0%, 1%, and 3.7% respectively. The minimal variance observed between the current simulation results and those reported in the literature (all below 5%) show that our results are suitable for methanol production.

4.5 Sensitivity analysis

4.5.1 Effect of temperature on the equilibrium TRM reactor product

The output of the TRM reactor comprises a mixture of H₂ and CO, residual reactants (CO₂, CH₄, and H₂O), as well as the non-reactive compound N₂. In Figure 13, the molar flow of significant gaseous products is plotted against reaction temperature, with H₂O/CH₄ ratio of 1.5 and a pressure of 1 atm. At 350 °C, the molar flow of H₂ initiates from zero and gradually increases and peaks at nearly 850 °C. Concurrently, the molar flow of CH₄ diminishes progressively to zero at 850 °C, indicating that CH₄ acts as a limiting reactant in the reactions.

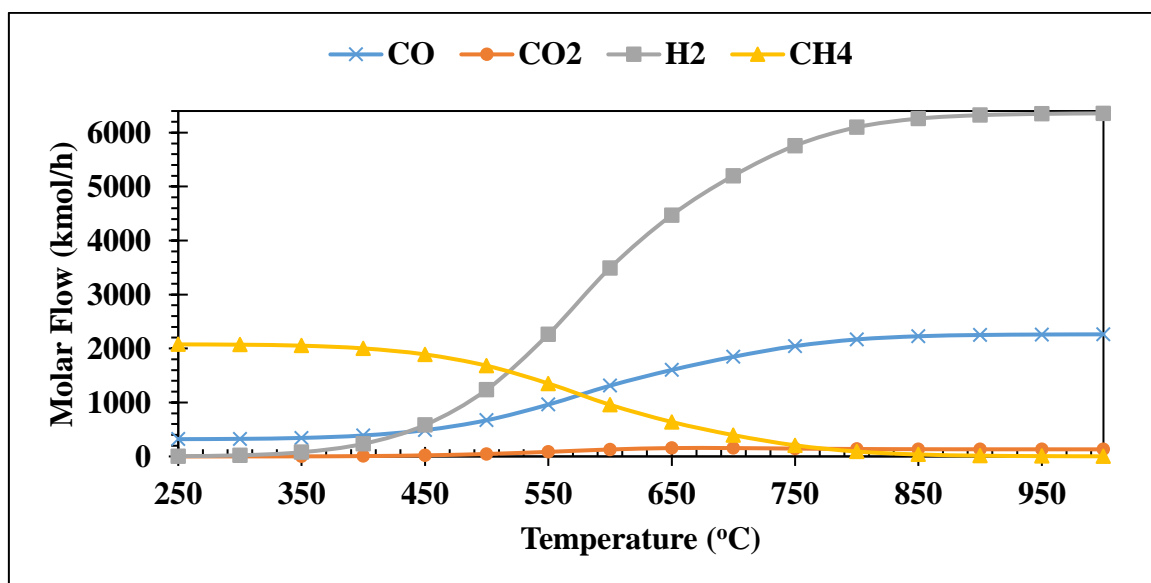


Figure 13: Effect of temperature on the equilibrium TRM reactor product.

Between 350 °C and 750 °C, there is a gradual rise in the molar flow of CO₂. This increase is attributed to the Water Gas Shift (WGS) reaction, which generates both CO₂ and H₂ by consuming CO in the presence of H₂O. Beyond 750 °C, the molar flow of CO₂ begins to decline, indicating its consumption through the DRM reaction. At 250 °C, the amount of generated CO is evident, showing an increase in its molar flow as the temperature rises, peaking at 850 °C.

The DRM and SRM processes reactions given by equations (2.1) and (2.3) involve the conversion of CO_2 and CH_4 into H_2 and CO . These processes are characterized as endothermic, indicating that higher temperatures promote the formation of products (H_2 and CO), aligning with Le Chatelier's principle and confirmed through the graph presented in Figure 13, which indicates that as the temperature rises, there is a corresponding increase in the molar flow of CO and H_2 . The syngas production simulation performed by Zhang et al. (2013), Song and Pan (2004), (Sun et al., 2010) and Santos et al. (2018) also demonstrates a comparable trend.

Observing the reactions involved in DRM and SRM, it becomes evident that the utilization of CH_4 serves as the primary source for H_2 production. With rising temperatures, the molar flow of H_2 consistently increases, while that of CH_4 decreases, showing a direct correlation between CH_4 consumption and H_2 generation.

Consequently, a higher CH_4 content in the TRM reactor feed leads to augmented H_2 production and an elevated H_2/CO ratio in the resultant syngas. Conversely, an increased CO_2 content in the TRM reactor feed enhances CO production, resulting in a lower H_2/CO ratio in the produced syngas.

4.5.2 Effect of the $\text{H}_2\text{O}/\text{CH}_4$ ratio in the TRM reactor and pressure on the produced syngas quality

The quality of the syngas produced depends on the molar ratio of H_2/CO . A very low H_2/CO ratio in the produced syngas indicates poor quality. Figure 14 illustrates the relationship between the H_2/CO ratio at the TRM reactor outlet and the $\text{H}_2\text{O}/\text{CH}_4$ ratio of the feed entering the reactor, varying pressure. This is done at a constant temperature of $850\text{ }^\circ\text{C}$ and pressures of 1 atm, 5 atm, and 10 atm. The variations in the $\text{H}_2\text{O}/\text{CH}_4$ ratio are achieved by maintaining a constant CH_4 molar flow and progressively increasing the H_2O molar flow in the TRM reactor feed.

Inspecting Figure 14 at a pressure of 10 atm, it becomes apparent that at $\text{H}_2\text{O}/\text{CH}_4$ ratio of 0.15, significant syngas production occurs with an H_2/CO molar ratio of 1.5, which progressively rises with the increasing $\text{H}_2\text{O}/\text{CH}_4$ ratio. The same trend is observed at pressures of 5 atm and 1 atm.

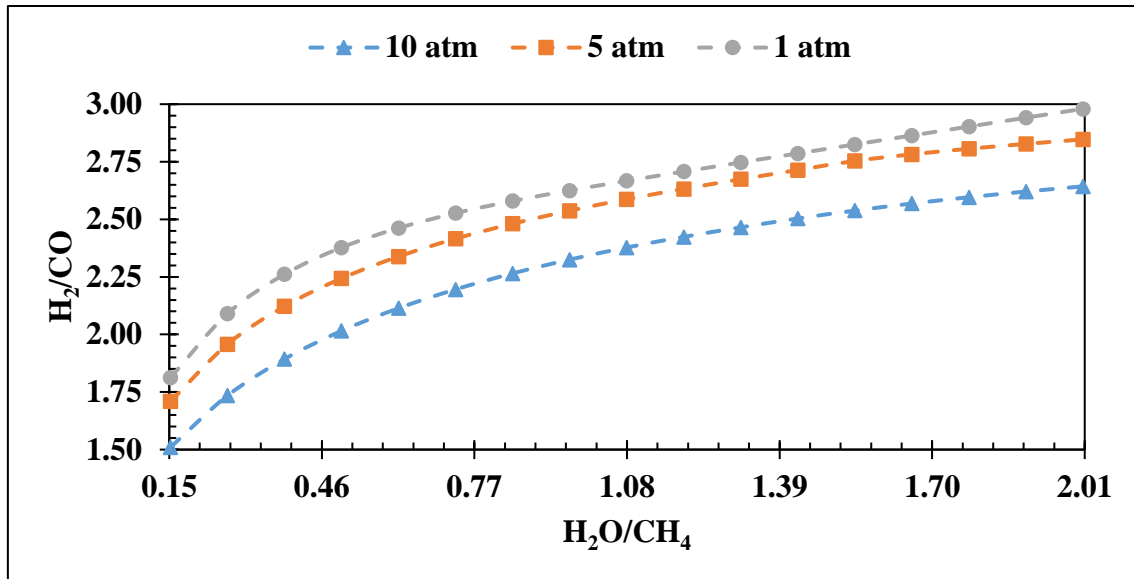


Figure 14: Effect of the H₂O/CH₄ ratio in the TRM reactor and pressure on the quality of the produced syngas.

Consequently, it is deduced that as the H₂O/CH₄ ratio increases in the TRM reactor feed, the H₂/CO ratio also increases in the produced syngas. This phenomenon aligns with the findings of Osat and Shojaati (2022) and is attributed to H₂O, which through the SRM reaction, acts as one of the sources of H₂ in the produced syngas. Thus, increments of H₂O in the feed result in increased H₂, consequently positively impacting the quality of the produced syngas by enhancing the H₂/CO ratio.

In the plots of pressures 1 atm, 5 atm and 10 atm; a consistent increase in the H₂/CO ratio in the produced syngas is observed as the H₂O/CH₄ ratio in the TRM reactor feed increases. However, the plot corresponding to the lowest pressure of 1 atm exhibits higher values of H₂/CO at a given H₂O/CH₄ ratio compared to the charts at 5 atm and 10 atm. This suggests that lower pressure in the TRM reactor promotes the formation of H₂ and CO. This phenomenon is in accordance with the results obtained by Dwivedi et al. (2017), Osat and Shojaati (2022), Manenti et al. (2015) and Dwivedi et al. (2016).

In the studies conducted by Osat and Shojaati (2022) and Dwivedi et al. (2016), the exact H₂/CO ratio in the produced syngas is not specified as it is in the simulation results of the current work. However, they show the conversion rates of CH₄, CO₂, and H₂O, which decrease with increasing pressure. Additionally, the results reported by (Manenti et al., 2015), based on experiments, further validate the findings of this work.

This observation also aligns with the Le Chatelier’s principle, which states that lowering the system pressure favors gas-phase reactions that result in a higher number of generated molecules of the products. This principle applies has been shown by the equations (2.1) and (2.3). These equations, generate more molecules of products H₂ and CO compared to the molecules consumed of the reactants CH₄, CO₂, and H₂O.

4.5.3 Effect of the pressure on the output of the MeOH reactor

The output of the MeOH reactor includes a mixture of CH₃OH and H₂O, residual reactants (CO, CO₂ and H₂), as well as the non-reactive compounds CH₄ and N₂. Figure 15 illustrates the molar flow of the main gaseous products plotted against pressure, at a constant temperature of 220 °C and a H₂/CO ratio of 2.81 in the syngas stream supplied to the MeOH reactor.

At 1 atm, the molar flow of CH₃OH is zero and gradually increases with increasing pressure until it reaches a peak of nearly 2200 kmol/h at a pressure of 50 atm. At this point, the molar flow remains constant with increasing pressure, simultaneously, the molar flow of H₂ gradually decreases to nearly 1250 kmol/h at 50 atm, while the molar flow of CO and CO₂ decreases to approximately zero at nearly 40 atm.

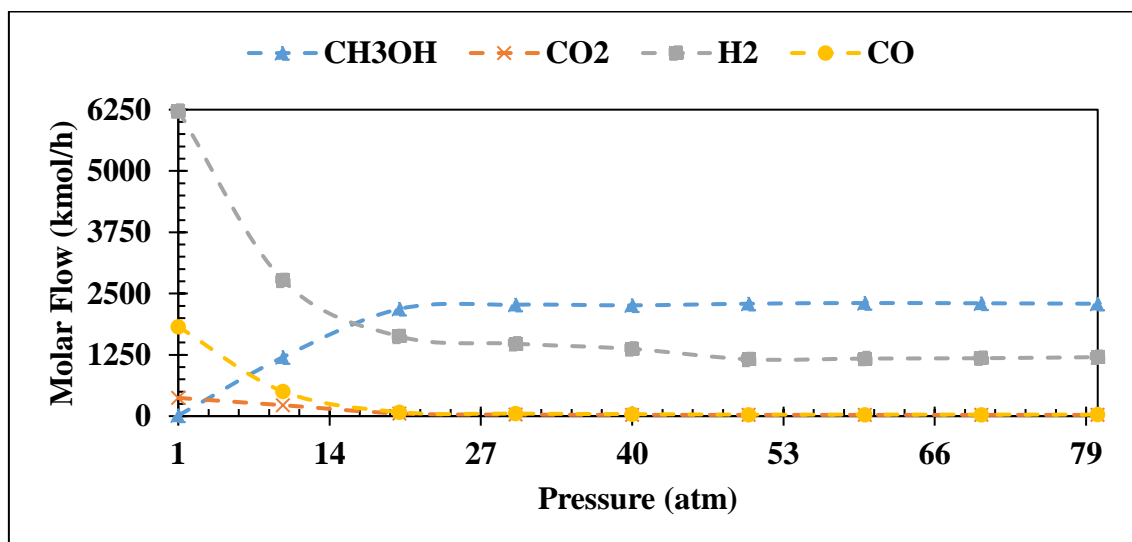


Figure 15: Effect of the pressure on the output of the MeOH reactor.

Overall, the chart indicates that an increase in pressure promotes the consumption of the reactants CO₂, CO, and H₂, thereby facilitating the formation of CH₃OH. This observation is consistent with Le Chatelier’s principle, which asserts that raising the system pressure favors gas-phase reactions that result in a lower number of generated molecules of the products. This principle is applicable to equations (2.9) and (2.10), which yield fewer

product molecules of CH₃OH and H₂O compared to the molecules consumed of reactants H₂, CO₂, and CO.

This trend is also evident in the methanol production simulation findings reported by Luyben (2010), Poto et al. (2022) and Chang et al. (2017). However, in the findings of Luyben (2010), the CH₃OH molar flow continues to increase progressively beyond 50 atm. This discrepancy arises because Luyben (2010) employed an operational temperature of 150 °C for the MeOH reactor.

In the developed simulation, at the temperature of 150 °C, lower molar flow rates of CH₃OH production are observed for a given syngas H₂/CO ratio and pressure compared to the molar flow of CH₃OH that would result from a temperature of 220 °C. The section 4.5.5 will provide a detailed explanation of the effect of MeOH reactor temperature on the quantities of CH₃OH produced.

4.5.4 Effect of the pressure on the amount of methanol vented

Venting gas into the atmosphere is common practice in chemical processing Plants. This is done primarily to prevent a sudden increase in pressure in the equipment or unit that could compromise its integrity and endanger personnel.

Figure 16 depicts the correlation between the molar flow of CH₃OH vented and the pressure employed in the MeOH reactor. This is done at a constant temperature of 220 °C and syngas H₂/CO molar ratio of 2.81 supplied to the reactor. The quantity of CH₃OH released is the portion that does not enter the distillation column and therefore discharged into the atmosphere via the stream labeled "VENT" in the PFD presented in section 4.3 (Figure 11).

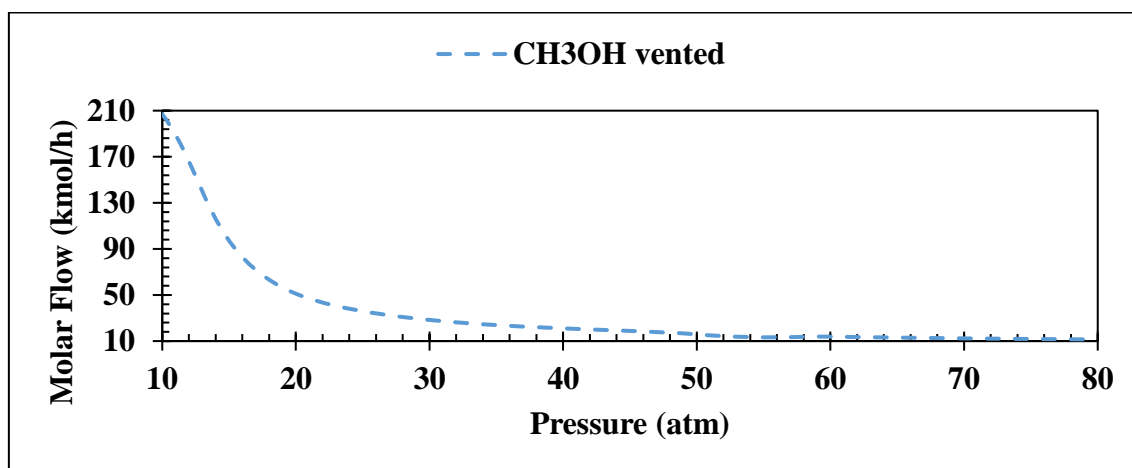


Figure 16: Effect of the pressure on the amount of methanol vented.

At 10 atm, a significant molar flow of CH₃OH develops, then start to decrease with increase in pressure until nearing a constant value of around 10 kmol/h. In general, it can be deduced that higher pressures in the MeOH reactor lead to a reduction in the molar flow of CH₃OH vented. This is preferable because minimizing the losses of CH₃OH in the VENT stream is necessary for the methanol production Plant.

4.5.5 Effect of the temperature on the produced methanol

Exothermic reactions are chemical processes that release energy into the environment, usually in the form of heat, causing the temperature to rise. These reactions are generally more favored at lower temperatures. Figure 17 illustrates the relationship between the MeOH reactor temperature and the molar flow of methanol produced. This analysis is conducted under a constant pressure of 50 atm and a syngas H₂/CO molar ratio of 2.81 supplied to the reactor.

At 200 °C, a significant molar flow of CH₃OH is evident, exhibiting a gradual increase with rising temperature until it peaks around 220 °C. Between 220 °C and 300 °C, there is a slight decrease in the molar flow of CH₃OH. However, beyond 300 °C, there is a notable sharp decline, resulting in a minimum constant value of nearly 70 kmol/h for the CH₃OH molar flow at temperatures exceeding 370 °C. The same trend is noticed in the work by C2.

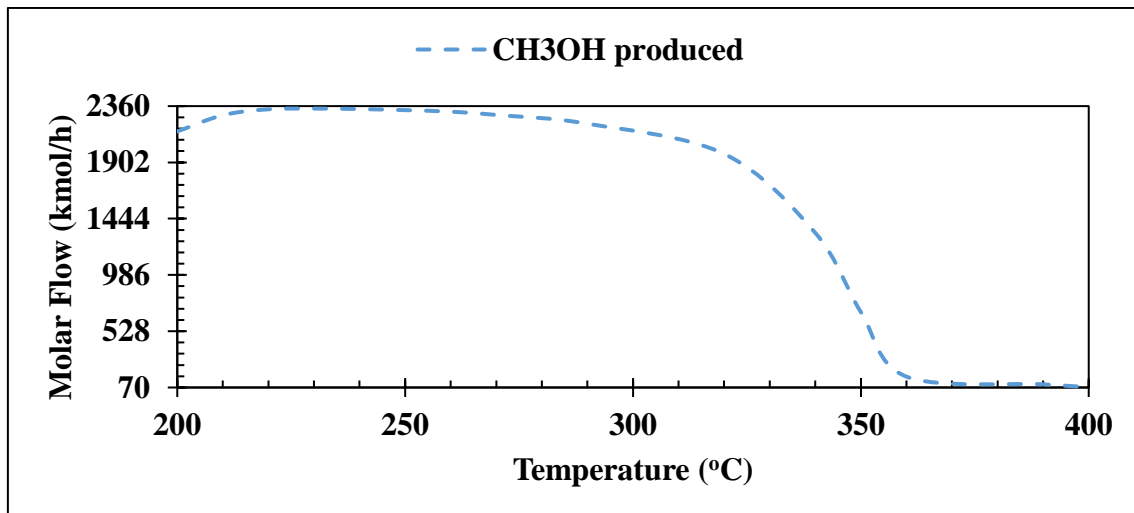


Figure 17: Effect of the temperature on the produced methanol.

Overall, it is deduced that beyond 220 °C, higher reaction temperatures lead to a reduction in CH₃OH production. This aligns with Fan et al. (2017), Poto et al. (2022) and Nyári et al. (2022) findings, which suggest that the exothermic nature of the CH₃OH production

reaction, involving CO, H₂, and CO₂ as reactants, makes it unfavorable at elevated temperatures.

Before 220 °C, higher reaction temperatures result in an increase in CH₃OH production, indicating that, in this range, the increase in temperatures favors the reaction, even though it is exothermic. This can be explained by the fact that the CH₃OH production reaction is not spontaneous at 50 atm and low temperature (e.g. 25 °C), meaning that the reactants do not naturally convert into products under these conditions without an external energy input.

Understanding this, it is deduced that the production reaction of CH₃OH occurs when there is an input of energy, which manifests as an increase in temperature.

4.5.6 Effect of the syngas H₂/CO ratio on the produced methanol

The syngas H₂/CO ratio is considered one of the key parameters in methanol production because it indicates the available H₂ to react with CO, as well as CO₂ present in the MeOH reactor feed. Figure 18 shows how the molar flow of produced methanol changes with the H₂/CO molar ratio in the syngas supplied to the MeOH reactor.

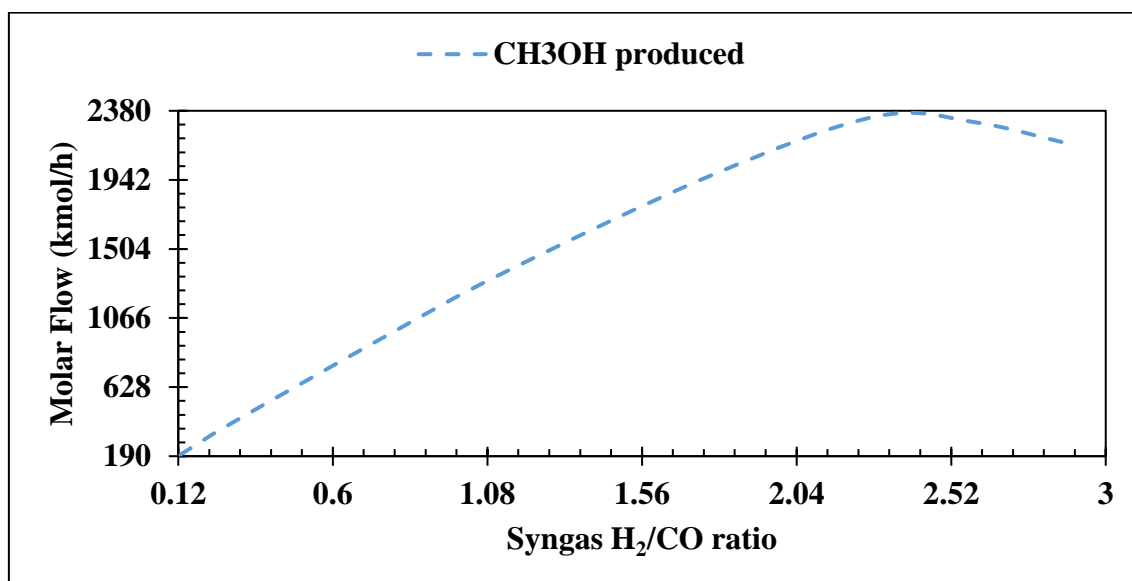


Figure 18: Effect of the syngas H₂/CO ratio on the produced methanol.

This analysis is performed under constant conditions a pressure of 50 atm and a temperature of 220 °C as the operational parameters for the reactor. At a syngas H₂/CO ratio of 0.12, there is a noticeable CH₃OH molar flow, which increases as the syngas H₂/CO ratio rises, reaching its peak at approximately 2.38. Beyond a H₂/CO ratio of 2.38,

it becomes apparent that further increases in the H₂/CO ratio result in a decrease in the CH₃OH molar flow.

In general, it can be inferred that an increase in the H₂/CO ratio leads to an increase in the CH₃OH molar flow up to a certain limit, after which the CH₃OH production begins to decrease since large quantities of H₂O will be present in the MeOH reactor, which will favor the reverse reaction described in equation (2.10), consuming CH₃OH and producing CO₂ and H₂.

4.6 Plant energy consumption and heat integration

Heat integration is a strategy that enhances energy efficiency and reduces environmental impact since heating and cooling process streams in chemical Plants typically require burning fossil fuels, which emit large quantities of greenhouse gases. Heat integration in methanol production Plants is an effective way to enhance process efficiency both environmentally and economically.

The total energy required for the simulated Plant, covering both the methane tri-reforming for syngas production and the methanol production sections, amounts to 1500 GJ/h as can be seen in the Figure 19.

Figure 19 depicts the energy needed for heating and cooling the process streams individually, which accounts for both cold and hot utilities. The black line indicates the energy needed to heat the cold streams which amounts 500 GJ/h, while the blue line represents the energy required to cool the hot streams which amounts 1000 GJ/h.

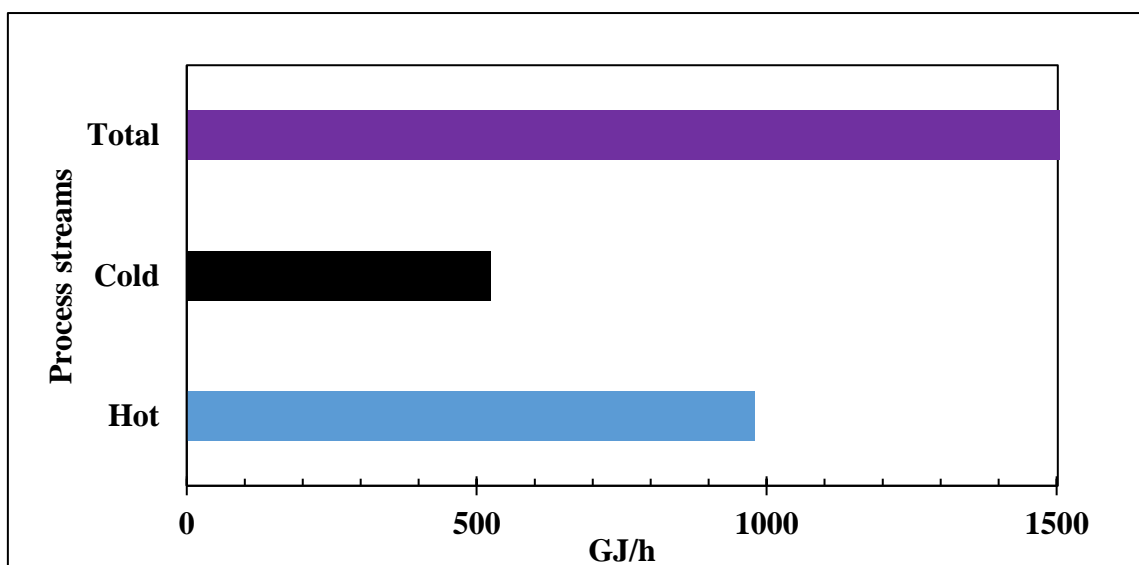


Figure 19: Plant energy consumption for heating and cooling process streams.

The total energy required for heating the process streams in the entire Plant can be reduced from the current 500 GJ/h to 12 GJ/h, as shown in Figure 20, which indicates a reduction of 97.6%. Similarly, the total energy required for cooling the process streams can be reduced from the current 1000 GJ/h to 423 GJ/h, as shown in Figure 21, reflecting a reduction of 57.7% by the implementation of Heat Exchanger Network (HEN).

Overall, the energy required for cooling the Plant's process streams is greater than the energy required for heating them, both before and after the implementation of HEN.

In order to enhance the energy efficiency of the Plant, aiming to reduce the need for cooling and heating energy, the hot and cold streams within the Plant are integrated into a HEN where the minimum constant temperature interval of 10 °C has been employed through the use of the Aspen Energy Analyzer (AEA) tool.

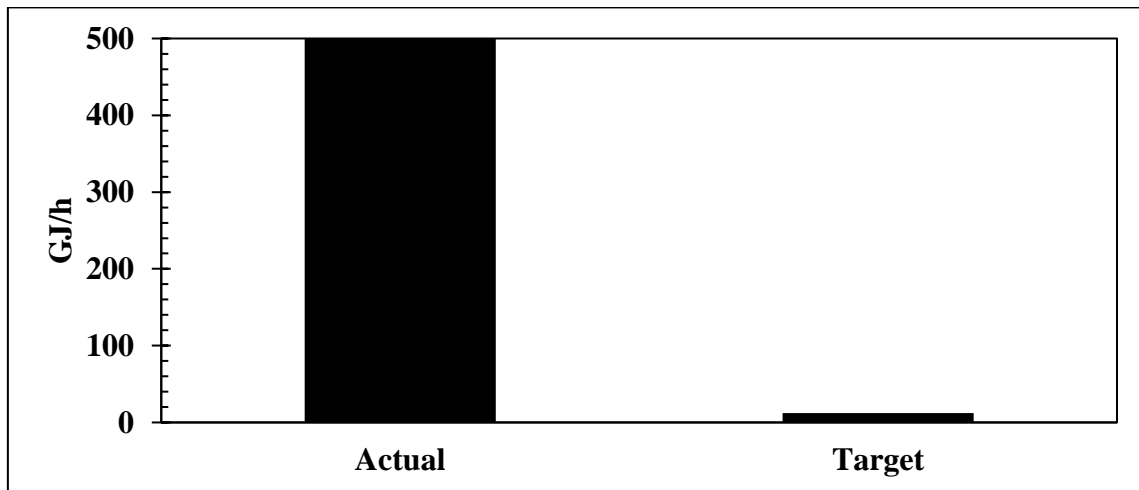


Figure 20: Actual and planned heating utilities for the Plant.

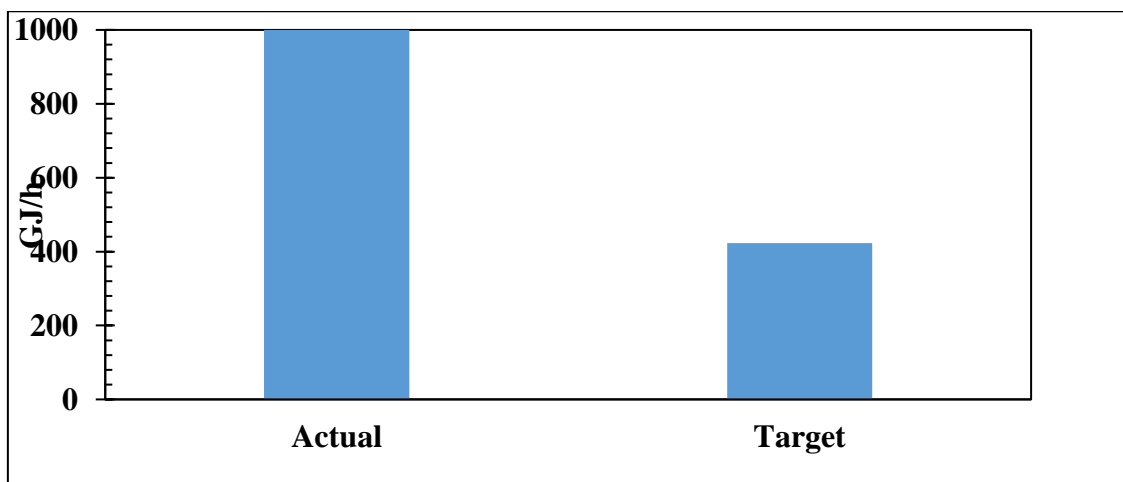


Figure 21: Actual and planned cooling utilities for the Plant.

Among the various HEN design diagrams generated using the AEA tool, the most suitable HEN diagram was selected based on the cost of acquiring the required heat exchangers, the number of heat exchangers, and the heat transfer area.

Figure 22 illustrates the chosen HEN diagram configuration after optimization to achieve the lowest possible cost invested, where blue dots indicate where the cold utility (cold water) at 15 °C cools the hot process streams labeled "To C5," "To C2," and "2." Red dots mark where the hot utility (HP steam) at 860 °C heats the cold process stream labeled "To H2." Grey dots represent the points of interaction between the hot and cold process streams.

The HEN diagram shows the interaction between the process and utility streams within the corresponding heat exchanger. Specifically, the process stream labeled "To C2" which is hot and needs to be cooled from 450 °C to 189 °C, is brought into contact with the process stream labeled "0" which is cold and needs to be heated from 137.6 °C to 182.6 °C, through the heat exchanger labeled "E-105" as depicted in Table 10. The total heat exchanged between the process streams "To C2" and "0" about 360 kJ/hm²C, as shown in Table 9.

The desired final temperature for cooling the process stream "To C2" is around 25 °C, but this cannot be achieved using the heat exchanger "E-105" with the cold stream "0." This problem is resolved by using another heat exchanger, "E-114," which further cools the "To C2" stream (now at 189 °C) by using cold utility water that is heated from 15 °C to 24.5 °C. The total heat transferred between the process stream "To C2" and the cold utility "cold water" is about 684 kJ/hm²C.

The process stream "Water 1," which needs to be heated from 25 °C to 100 °C to produce steam, is brought into contact with the hot process stream "2," which needs to be cooled from 219 °C to 170.4 °C through the heat exchanger "E-108" as shown in Table 10. The overall heat transferred between the process streams "2" and "Water 1" is about 360 kJ/hm²C, as indicated in Table 9.

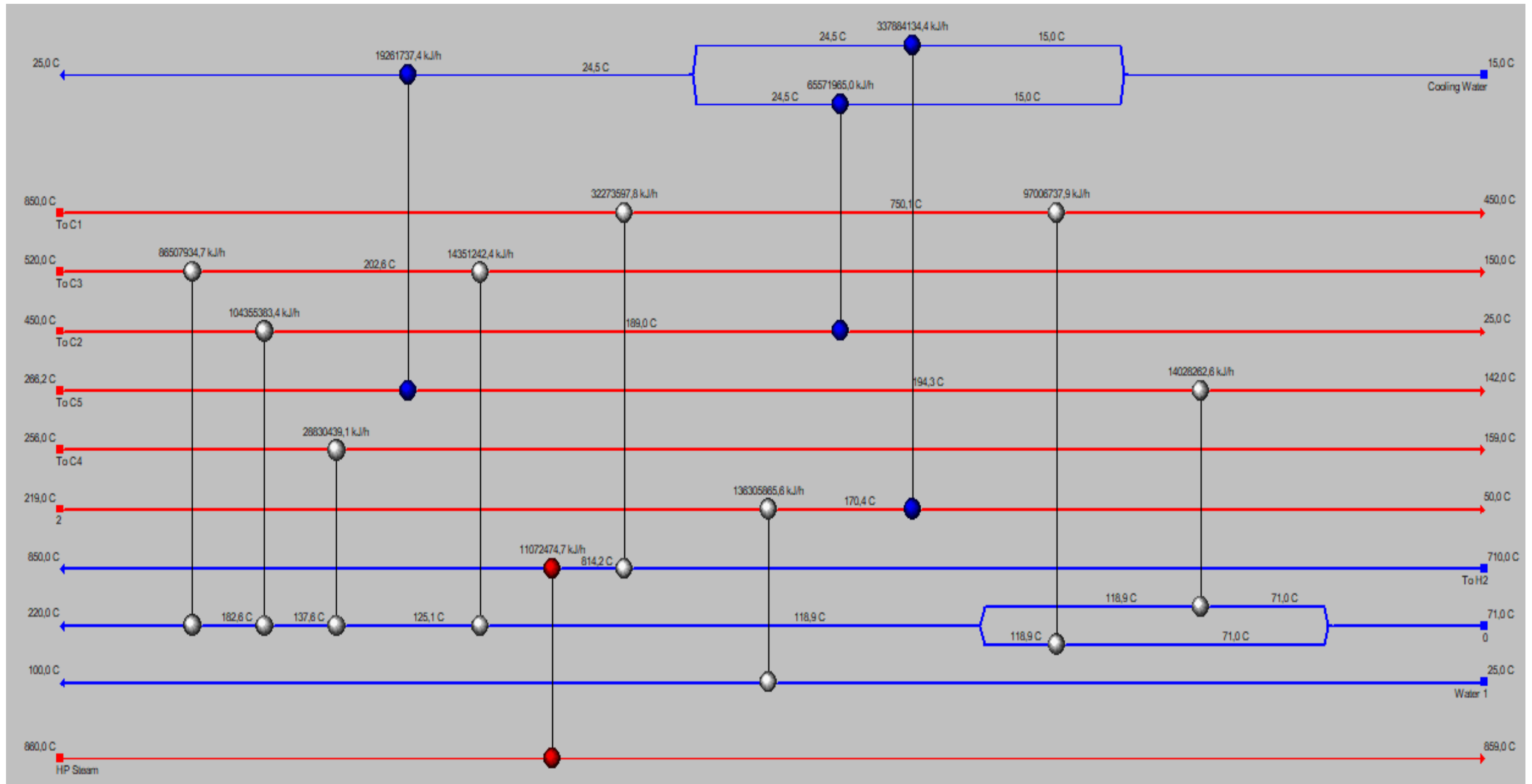


Figure 22: Plant HEN diagram.

The heat transferred in the heat exchanger "E-108" is sufficient to vaporize the process stream "Water 1," eliminating the need for an additional heat exchanger. In contrast, with the process stream "To C2," which requires cooling from 450 °C to 25 °C, two heat exchangers, "E-105" and "E-114," are employed for this purpose.

The same principle applied to describe how the process stream "To C2" is cooled down and the process stream "Water 1" is heated up, as mentioned earlier, is applicable to the other streams involved in the Plant.

Table 9 presents data on the energy flow rates, surface areas utilized, and the total heat exchanged in each heat exchanger configured through the HEN. Conversely, Table 10 provides details regarding the process and utility streams involved, including their respective temperatures at each heat exchanger.

Table 9: Heat exchangers features from the designed HEN.

Heat Exchanger	Load (kJ/h)	Area (m ²)	Overall U (kJ/hm ² C)
E-103	86,507,935	2,510	360
E-106	19,261,737	139	684
E-110	14,351,242	803	360
E-112	97,006,738	551	360
E-104	11,072,475	694	697
E-105	104,355,383	2,457	360
E-107	28,830,439	1,248	360
E-109	32,273,598	2,976	360
E-111	14,028,263	581	360
E-108	136,305,866	2,981	360
E-114	65,571,965	1,813	684
E-113	337,884,134	6,603	684

Table 10: Process and utility streams features from the designed HEN.

Heat Exchanger	Hot Stream	Hot T in (°C)	Hot T out (°C)	Cold Stream	Cold T in (°C)	Cold T out (°C)
E-103	To C3	520.0	202.6	0	182.6	220.0
E-106	To C5	266.2	194.3	C. Water	24.5	25.0
E-110	To C3	202.6	150.0	0	118.9	125.1
E-112	To C1	750.1	450.0	0	71.0	118.9
E-104	HP Steam	860.0	859.0	To H2	814.2	850.0
E-105	To C2	450.0	189.0	0	137.6	182.6
E-107	To C4	256.0	159.0	0	125.1	137.6
E-109	To C1	850.0	750.1	To H2	710.0	814.2
E-111	To C5	194.3	142.0	0	71.0	118.9
E-108	2	219.0	170.4	Water 1	25.0	100.0
E-114	To C2	189.0	25.0	C. Water	15.0	24.5
E-113	2	170.4	50.0	C. Water	15.0	24.5

Before the implementation of HEN, the total duty required for heating and cooling Plant’s process streams was estimated at 1500 GJ/h. Following the implementation of HEN, the total energy requirement decreased to 435 GJ/h, resulting in gross energy savings of 71%, as illustrated in Figure 23.

Figure 23 illustrates the energy savings achieved by implementing HEN. In this setup, heat exchangers are engineered to facilitate the generation of both cold and hot process streams without the need for coolers and heaters, which typically consume energy, be it thermal or electrical.

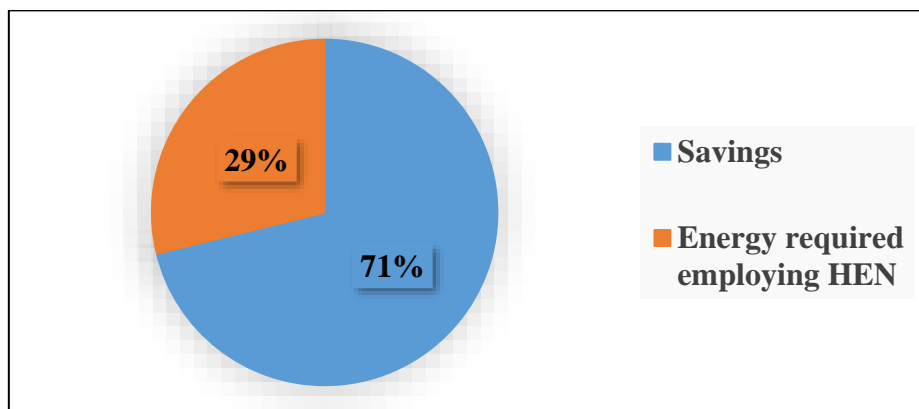


Figure 23: Amount of energy saved after the designed HEN.

4.7 Economic assessment

As explained in the syngas production results section, a significant disagreement from previous studies, such as that conducted by Zhang et al. (2013), Kim et al. (2010), Borreguero et al. (2020) and Dwivedi et al. (2016), lies in the utilization of pre-reactors to supply energy to the TRM reactor. These pre-reactors not only produce CO₂ and H₂O for the process but also eliminate heavier hydrocarbons that could potentially deactivate the Ni/Al₂O₃ catalyst in the TRM reactor.

Subsequently, the economic viability of the proposed Plant, encompassing both syngas and methanol production sections under the specified conditions following sensitivity analyses, will be assessed.

The initial phase of the economic evaluation involves estimating the acquisition cost of the equipment utilized in the Plant, relying on their primary dimensions or characteristic parameters. The acquisition cost of all equipment has been determined using the Aspen Process Economic Analyzer (APEA) tool provided by Aspen HYSYS and Aspen PLUS and it is shown in the Table 11.

The total costs for acquiring the main equipment listed in Table 11 are based on 2019 prices, as the software used for this economic analysis calculates and estimates costs using the equipment prices from that year. To update these values for the current year, 2024, the average global inflation rates shown in Figure 24 were applied to the product prices. Consequently, the final total cost for acquiring the main equipment was calculated to be US\$ 74,646,118.

After obtaining the main equipment acquisition cost, the fixed capital investment was determined using the percentage method outlined by Dueñas et al. (2010) resulting in a value of US\$ 302,764,655 as can be seen in Table 12. This figure takes into account the costs of purchasing chillers and heaters to be used in the Plant, i.e. without implementing HEN. With the implementation of HEN, which means eliminating the use of chillers and heaters to cool and heat the Plant process streams and using only heat exchangers for this, the fixed capital investment becomes US\$ 319,985,400 where the heat exchangers cost US\$ 7,576,669.

Table 11: Acquisition costs for the main equipment.

Equipment	Cost ₂₀₁₉	Description
K1	32,519,520	First compressor step of the produced syngas
K2	8,129,880	First compressor step of the produced syngas
K3	3,979,300	Third compressor step of the produced syngas
K4	3,791,500	Compressor of the recycle stream from F1
K5	1,396,700	Compressor of the recycle stream from F2
K6	1,028,700	Compressor of the recycle stream from F3
C1	191,000	Heat exchanger for cooling TRM reactor product
C2	25,100	Heat exchanger for cooling C1 outlet stream
C3	40,141	Heat exchanger for cooling K1 outlet stream
C4	18,459	Heat exchanger for cooling K2 outlet stream
C5	444,600	Heat exchanger for cooling MeOH reactor product
H1	90,900	Heat exchanger for steam generation
H2	65,600	Heat exchanger for heating the TRM reactor feed
H3	1,375,100	Heat exchanger heating the MeOH reactor feed
Pre-reactor 1	550,096	Reactor for heavier hydrocarbons combustion from NG
Pre-reactor 2	66,012	Reactor for heavier hydrocarbons combustion from LPFG
Pre-reactor 3	38,506	Reactor for heavier hydrocarbons combustion from HPFG
TRM reactor	71,939	Reactor for syngas production
MeOH reactor	371,043	Reactor for methanol production
F0	113,200	Flash vessel for water removal in the syngas produced
F1	196,700	First vessel step for lighter components removal in the methanol produced
F2	35,200	Second vessel step for lighter components removal in the methanol produced
F3	40,700	Third vessel step for lighter components removal in the methanol produced
DC	497,000	Distillation column for water removal in the methanol produced
Total	55,076,896	

Table 12 shows the fixed capital investment calculations for the Plant, which includes the syngas production and methanol production sections. The installation costs account for 60% of the total purchase costs for the main equipment used in the Plant. This includes the budget allocated to buildings, piping, electricity, insulation, painting and instrumentation and control.

Table 12: Results of the percentage method for fixed capital investment.

Item	Percentage (%)	Cost (US\$)
Main equipment costs (E)		74,646,118
Installations costs (M)	60%E	44,787,671
Buildings	28%	12,540,548
Piping	45%	20,154,452
Instrumentation and control	10%	4,478,767
Electricity	10%	4,478,767
Insulation	5%	2,239,384
Painting	2%	895,753
Detail engineering	15%(E+M)	17,915,068
Process engineering and licensing	20%(E+M)	23,886,758
Construction	50%(E+M)	59,716,894
Construction supervision	10%(E+M)	11,943,379
ISBL		232,895,888
Auxiliary services and catalyst inventory	4% ISBL	9,315,836
Construction expenses	8% ISBL	18,631,671
Contractor's fee	3% ISBL	6,986,877
Contingency	15% ISBL	34,934,383
Fixed capital investment		302,764,655

In addition to installation costs, Table 12 also presents the calculations for detailed engineering, process engineering and licensing, construction, and construction supervision costs. These costs are all based on the total cost of the main equipment and their installation. The table also shows the cost of the Inside Battery Limits (ISBL), which includes the cost of purchasing and installing all the process equipment that constitutes the new Plant, as outlined by Towler and Sinnott (2022).

Figure 24 shows the different world average inflation rates for product prices applied from 2020 to the current year, 2024, which are positive, meaning that the prices charged for products acquisition increase over the years.

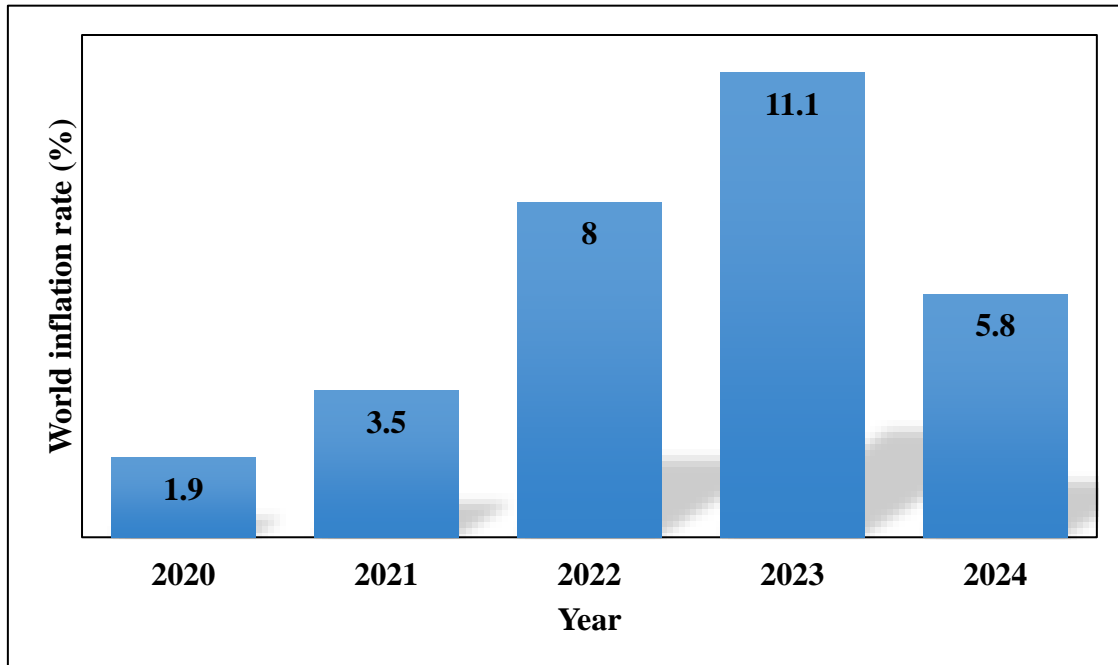


Figure 24: World average inflation rates of product prices.

The ISBL for this project was estimated based on the capacity of the syngas production section of 718,305 mtpa and the capacity of the methanol production section of 613,148 mtpa, assuming 8,000 operating hours per year. In addition, auxiliary services, construction costs, contractor's fees and contingency costs were calculated as a percentage of the cost of the ISBL.

Taking into account the previous study by Borreguero et al. (2020), Aromada et al. (2021) as well as Towler and Sinnott (2022), the indirect labor, payroll charges, and laboratory expenses were computed as 30%, 25%, and 20% of the direct labor, respectively. Conversely, maintenance, operating supplies, and property taxes and insurance were estimated at 3%, 5%, and 1% of the fixed capital investment, respectively.

The economic analysis methods most commonly used by many companies to make decisions about implementing projects include the Net Present Value (NPV), which is the sum of the present values of future cash flows, as well as the Internal Rate of Return (IRR), which is the discount rate that makes the NPV of all cash flows equal to zero.

The estimated NPV and IRR for the current project, taking into account the implementation of HEN, are about US\$ 440,183,674 and 17.3%, respectively. These calculations are based on the formulas described by Towler and Sinnott (2022) and López Prol and Steininger (2020), as shown by equations (2.24) and (2.25). The CF_n represents the cash flow in year n , t is the project life in years and i is the interest rate, set at 3.15% according to Standard Bank Mozambique (2024).

$$NPV = \sum_{n=1}^{n=t} \frac{CF_n}{(1+i)^n} \quad (2.24)$$

$$\sum_{n=1}^{n=t} \frac{CF_n}{(1+i)^n} = 0 \quad (2.25)$$

The estimated NPV for the current project, without considering the implementation of HEN, is approximately US\$ - 343,142,841. This negative value is undesirable because a project should be rejected if the NPV is less than zero and accepted if it is greater than zero. Therefore, it can be concluded that the current project is economically feasible when HEN is implemented.

The payback time for the budget to be invested in the current project, which includes both fixed capital investment and working capital, estimated through the Figure 25, is approximately 6 years. This timeframe is appropriate, as investments in most methanol production Plant projects are usually recovered within 4 to 7 years, as outlined by Towler and Sinnott (2022) and Borreguero et al. (2020).

Figure 25 shows the accumulated cash flow in millions (M) of US\$ over the life of the project. In year 0, the accumulated cash flow is – 347,000,000 US\$, which indicates that the project does not generate profits at that point. Over time, the accumulated cash flow gradually increases, remaining negative until the 5th year. After the 5th year, the accumulated cash flow becomes positive, which means that the project is generating profits and the entire invested budget has been recovered, and continues to increase steadily, reaching its maximum value in the 15th year.

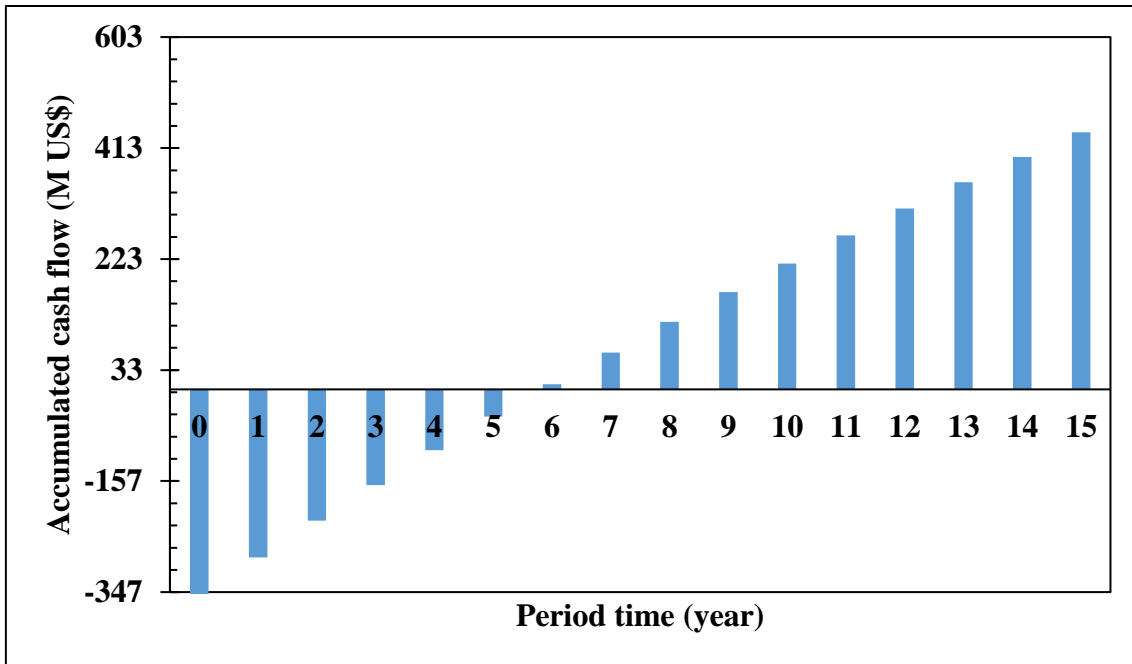


Figure 25: Accumulated cash flow over different years.

4.8 CO₂ reduction opportunity

In an era where the world is concerned about climate change due to rampant greenhouse gas emissions, the main contribution of this project is to reduce these emissions. Its implementation can result in 98% reduction of CO₂. These are emissions-equivalent to those that would be produced by burning the gas that is now proposed as a raw material for syngas production for methanol production. The estimated residual CO₂ emission of about 3400 t/a if the project is implemented (Figure 26) is obtained from the "VENT" stream shown in the methanol PFD.

Figure 26 depicts the estimated quantities of CO₂ equivalent emissions with and without the current project implementation, calculated using the global warming potential obtained in IPCC (2014).

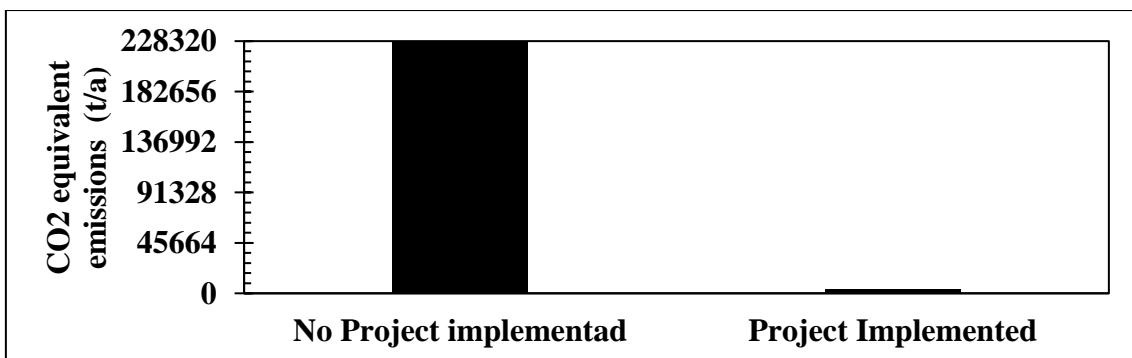


Figure 26: CO₂ equivalent emissions reduction with and no project implemented.

CHAPTER V

CONCLUSIONS AND RECOMMENDATIONS

5.1 Introduction

This work examined the production of methanol from syngas. The syngas was obtained through tri-reforming of methane from natural gas and flare gas. For this, Aspen HYSYS and Aspen PLUS were employed to simulate kinetic equations and plug flow reactors. On the basis of the simulation results, the main conclusions and recommendations, including the techno-economic analysis of the entire methanol production process are presented.

5.2 Conclusions

- The overall conversion rate of CH₄ into syngas suitable for methanol production is about 98.5%;
- The overall conversion rates of CO, CO₂, and H₂ into methanol are 99.5%, 93%, and 81%, respectively;
- The methanol produced has a purity of 98.5% by weight, a gross heating value of 22,315 kJ/kg, an API gravity of 45.8, a dew point temperature of 65.5 °C at 1 atm and a mass flow rate of 75433 kg/h;
- In general, high temperatures and low pressures favor the syngas production (SRM and DRM), and a high H₂O/CH₄ molar ratio in the tri-reforming reactor results in high H₂/CO molar ratios. Conversely, low temperatures and high pressures favor the methanol production (CO and CO₂ hydrogenation), and a high H₂/CO ratio in the syngas leads to high methanol production rates;
- The optimal operating conditions for syngas production in the TRM reactor are a pressure of 1 atm, a temperature of 850 °C, and an H₂O/CH₄ molar ratio of 1.5. For methanol production in the MeOH reactor, the optimal conditions are a pressure of 50 atm, a temperature of 220 °C, and a syngas H₂/CO ratio of 2.81;
- The implementation of HEN saves about 71% of the total energy required for heating and cooling the process streams in the Plant;
- With the implementation of HEN, the project's NPV is about US\$ 440,183,674, indicating that it is economically feasible, with a determined IRR of about 17.3%. Without HEN, the NPV drops to a negative value of US\$ -343,142,841, meaning the project does not generate profits under these conditions. This is due to the high

operating costs associated with the intensive electricity needed for running coolers and heaters without HEN.

5.3 Recommendations

For future research on modeling, simulating, and performing a techno-feasibility study of a methanol production plant using syngas derived from natural gas and incorporated flare gas, it is recommended to:

- Explore the potential economic advantages of reducing CO₂ emissions in the emerging global carbon credit market from the results obtained in the current research;
- Investigate methods to increase the CO₂ content in the produced syngas in order to enhance H₂ conversion during methanol production;
- Develop the process control systems for the entire proposed methanol Plant in the current research and create the corresponding Process and Instrumentation Diagrams (P&IDs);
- Investigate the techno-feasibility of producing dimethyl ether from methanol.

REFERENCES

- Alibrahim, H. A., Khalafalla, S. S., Ahmed, U., Park, S., Lee, C. J., & Zahid, U. (2021). Conceptual design of syngas production by the integration of gasification and dry-reforming technologies with CO₂ capture and utilization. *Energy Conversion and Management*, 244. <https://doi.org/10.1016/j.enconman.2021.114485>
- Al-Khori, K., Bicer, Y., Aslam, M. I., & Koç, M. (2021). Flare emission reduction utilizing solid oxide fuel cells at a natural gas processing plant. *Energy Reports*, 7, 5627–5638. <https://doi.org/10.1016/j.egy.2021.08.164>
- Anomohanran, O. (2012). Determination of greenhouse gas emission resulting from gas flaring activities in Nigeria. *Energy Policy*, 45, 666–670. <https://doi.org/10.1016/j.enpol.2012.03.018>
- Aromada, S. A., Eldrup, N. H., & Erik Øi, L. (2021). Capital cost estimation of CO₂ capture plant using Enhanced Detailed Factor (EDF) method: Installation factors and plant construction characteristic factors. *International Journal of Greenhouse Gas Control*, 110. <https://doi.org/10.1016/j.ijggc.2021.103394>
- Asadi, J., Yazdani, E., Hosseinzadeh Dehaghani, Y., & Kazempoor, P. (2021). Technical evaluation and optimization of a flare gas recovery system for improving energy efficiency and reducing emissions. *Energy Conversion and Management*, 236. <https://doi.org/10.1016/j.enconman.2021.114076>
- Ay, S., Ozdemir, M., & Melikoglu, M. (2021). Effects of metal promotion on the performance, catalytic activity, selectivity and deactivation rates of Cu/ZnO/Al₂O₃ catalysts for methanol synthesis. *Chemical Engineering Research and Design*, 175, 146–160. <https://doi.org/10.1016/j.cherd.2021.08.039>
- Bergougui, B. (2024). Moving toward environmental mitigation in Algeria: Asymmetric impact of fossil fuel energy, renewable energy and technological innovation on CO₂ emissions. *Energy Strategy Reviews*, 51. <https://doi.org/10.1016/j.esr.2023.101281>
- Borreguero, A. M., Dorado, F., Capuchino-Biezma, M., Sánchez-Silva, L., & García-Vargas, J. M. (2020). Process simulation and economic feasibility assessment of the methanol production via tri-reforming using experimental kinetic equations. *International Journal of Hydrogen Energy*, 45(51), 26623–26636. <https://doi.org/10.1016/j.ijhydene.2020.07.013>

- Bozzano, G., & Manenti, F. (2016). Efficient methanol synthesis: Perspectives, technologies and optimization strategies. In *Progress in Energy and Combustion Science* (Vol. 56, pp. 71–105). Elsevier Ltd. <https://doi.org/10.1016/j.pecs.2016.06.001>
- BR, B. R. (2021). *Publicação oficial da República de Moçambique – I SÉRIE – Número 212*. <https://doi.org/https://www.portaldogoverno.gov.mz/por/Governo/Legislacao/Boletins-da-Republica/Boletins-da-Republica-2021>
- Bussche, K. M. Vanden, & Froment, G. F. (1996). A Steady-State Kinetic Model for Methanol Synthesis and the Water Gas Shift Reaction on a Commercial Cu/ZnO/Al₂O₃ Catalyst. In *JOURNAL OF CATALYSIS* (Vol. 161).
- CA, C. A. (2024). *Track Oxygen Price Trend*. <https://doi.org/https://www.chemanalyst.com/Pricing-data/oxygen-1575>
- Carapellucci, R., & Giordano, L. (2020). Steam, dry and autothermal methane reforming for hydrogen production: A thermodynamic equilibrium analysis. *Journal of Power Sources*, 469. <https://doi.org/10.1016/j.jpowsour.2020.228391>
- Chafik, T. (2021). Towards harnessing local natural clay in power to X technologies: Review on syngas production using low cost catalyst extruded as honeycomb monolith. *Materials Today: Proceedings*, 37, 3834–3839. <https://doi.org/10.1016/j.matpr.2020.08.403>
- Chang, K., Wang, T., & Chen, J. G. (2017). Hydrogenation of CO₂ to methanol over CuCeTiO_x catalysts. *Applied Catalysis B: Environmental*, 206, 704–711. <https://doi.org/10.1016/j.apcatb.2017.01.076>
- De La Osa, A. R., De Lucas, A., Romero, A., Valverde, J. L., & Sánchez, P. (2011). Kinetic models discrimination for the high pressure WGS reaction over a commercial CoMo catalyst. *International Journal of Hydrogen Energy*, 36(16), 9673–9684. <https://doi.org/10.1016/j.ijhydene.2011.05.043>
- Dinani, A. M., Nassaji, A., & Hamzehlouyan, T. (2023a). An optimized economic-environmental model for a proposed flare gas recovery system. *Energy Reports*, 9, 2921–2934. <https://doi.org/10.1016/j.egyr.2023.01.103>

- Dinani, A. M., Nassaji, A., & Hamzehlouyan, T. (2023b). An optimized economic-environmental model for a proposed flare gas recovery system. *Energy Reports*, 9, 2921–2934. <https://doi.org/10.1016/j.egy.2023.01.103>
- Dueñas, L., Martínez, A., Fernández, F., & Marcos, M. (2010). *Metodologías de diseño aplicado y gestión de proyectos para ingenieros químicos* (C. Meléndez, Ed.; 3rd ed.). Servicio de Publicacions de la Universidad de Castilla-La Mancha.
- Dwivedi, A., Gudi, R., & Biswas, P. (2016). Sensitivity based optimization of the Tri-reforming based CO₂ valorization process. *IFAC-PapersOnLine*, 49(7), 359–364. <https://doi.org/10.1016/j.ifacol.2016.07.362>
- EDM, E. de M. (2024). *Electricity Tariffs*. <https://doi.org/https://www.edm.co.mz/en/website/page/electricity-tariffs>
- EIA, E. I. A. (2024). *Natural Gas Industrial Price*. <https://doi.org/https://www.eia.gov/dnav/ng/hist/n3035us3m.htm>
- Elvidge, C. D., Zhizhin, M., Baugh, K., Hsu, F. C., & Ghosh, T. (2016). Methods for global survey of natural gas flaring from visible infrared imaging radiometer suite data. *Energies*, 9(1). <https://doi.org/10.3390/en9010014>
- Fan, R., Kyodo, M., Tan, L., Peng, X., Yang, G., Yoneyama, Y., Yang, R., Zhang, Q., & Tsubaki, N. (2017). Preparation and application of Cu/ZnO catalyst by urea hydrolysis method for low-temperature methanol synthesis from syngas. *Fuel Processing Technology*, 167, 69–77. <https://doi.org/10.1016/j.fuproc.2017.06.026>
- Farniaei, M., Abbasi, M., Rahnama, H., Rahimpour, M. R., & Shariati, A. (2014). Syngas production in a novel methane dry reformer by utilizing of tri-reforming process for energy supplying: Modeling and simulation. *Journal of Natural Gas Science and Engineering*, 20, 132–146. <https://doi.org/10.1016/j.jngse.2014.06.010>
- Fazlikeshteli, S., Vendrell, X., & Llorca, J. (2024). Catalytic partial oxidation of methane over bimetallic Ru–Ni supported on CeO₂ for syngas production. *International Journal of Hydrogen Energy*, 51, 1494–1507. <https://doi.org/10.1016/j.ijhydene.2023.07.349>

- Fedorova, Z. A., Danilova, M. M., & Zaikovskii, V. I. (2020). Porous nickel-based catalysts for tri-reforming of methane to synthesis gas: Catalytic activity. *Materials Letters*, 261. <https://doi.org/10.1016/j.matlet.2019.127087>
- From, T. N., Partoon, B., Rautenbach, M., Østberg, M., Bentien, A., Aasberg-Petersen, K., & Mortensen, P. M. (2024). Electrified steam methane reforming of biogas for sustainable syngas manufacturing and next-generation of plant design: A pilot plant study. *Chemical Engineering Journal*, 479. <https://doi.org/10.1016/j.cej.2023.147205>
- Galadima, A., & Muraza, O. (2015). From synthesis gas production to methanol synthesis and potential upgrade to gasoline range hydrocarbons: A review. In *Journal of Natural Gas Science and Engineering* (Vol. 25, pp. 303–316). Elsevier B.V. <https://doi.org/10.1016/j.jngse.2015.05.012>
- Graaf, G. H., Stamhuis, E. J., & Beenackersz, A. A. C. M. (1988). KINETICS OF LOW-PRESSURE METHANOL SYNTHESIS. In *Chemical Engineering Science* (Vol. 43, Issue 12).
- Guamán-Marquines, C. W., Mendoza-Loor, R. J., Gómez-Salcedo, Y., & Baquerizo-Crespo, R. J. (2023). Assessment of the start-up of tubular reactors on a laboratory scale for the anaerobic digestion of slaughterhouse wastewater. *International Journal of Thermofluids*, 19. <https://doi.org/10.1016/j.ijft.2023.100378>
- Hamidzadeh, Z., Sattari, S., Soltanieh, M., & Vatani, A. (2020). Development of a multi-objective decision-making model to recover flare gases in a multi flare gases zone. *Energy*, 203. <https://doi.org/10.1016/j.energy.2020.117815>
- Hasanat, A. U., Khoja, A. H., Naeem, N., Al-Anazi, A., Liaquat, R., Khan, B. A., & Din, I. U. (2023). Thermocatalytic partial oxidation of methane to syngas (H₂, CO) production using Ni/La₂O₃ modified biomass fly ash supported catalyst. *Results in Engineering*, 19. <https://doi.org/10.1016/j.rineng.2023.101333>
- Heidari, M., Ataei, A., & Rahdar, M. H. (2016). Development and analysis of two novel methods for power generation from flare gas. *Applied Thermal Engineering*, 104, 687–696. <https://doi.org/10.1016/j.applthermaleng.2016.05.099>
- IPCC. (2014). *Fifth Assessment Synthesis Report*. <https://doi.org/https://ar5-syr.ipcc.ch/index.php>

- Katebah, M., Al-Rawashdeh, M., & Linke, P. (2022). Analysis of hydrogen production costs in Steam-Methane Reforming considering integration with electrolysis and CO₂ capture. *Cleaner Engineering and Technology*, 10. <https://doi.org/10.1016/j.clet.2022.100552>
- Khajeh, S., Arab Aboosadi, Z., & Honarvar, B. (2014). A comparative study between operability of fluidized-bed and fixed-bed reactors to produce synthesis gas through tri-reforming. *Journal of Natural Gas Science and Engineering*, 19, 152–160. <https://doi.org/10.1016/j.jngse.2014.05.005>
- Khalili-Garakani, A., Nezhadfar, M., & Iravaninia, M. (2022). Enviro-economic investigation of various flare gas recovery and utilization technologies in upstream and downstream of oil and gas industries. *Journal of Cleaner Production*, 346. <https://doi.org/10.1016/j.jclepro.2022.131218>
- Khanipour, M., Mirvakili, A., Bakhtyari, A., Farniaei, M., & Rahimpour, M. R. (2020). A membrane-assisted hydrogen and carbon oxides separation from flare gas and recovery to a commercial methanol reactor. *International Journal of Hydrogen Energy*, 45(12), 7386–7400. <https://doi.org/10.1016/j.ijhydene.2019.04.149>
- Kim, I. H., Kim, S., Cho, W., & Yoon, E. S. (2010). Simulation of commercial dimethyl ether production plant. *Computer Aided Chemical Engineering*, 28(C), 799–804. [https://doi.org/10.1016/S1570-7946\(10\)28134-8](https://doi.org/10.1016/S1570-7946(10)28134-8)
- López Prol, J., & Steininger, K. W. (2020). Photovoltaic self-consumption is now profitable in Spain: Effects of the new regulation on prosumers' internal rate of return. *Energy Policy*, 146. <https://doi.org/10.1016/j.enpol.2020.111793>
- Luyben, W. L. (2010). Design and control of a methanol reactor/column process. *Industrial and Engineering Chemistry Research*, 49(13), 6150–6163. <https://doi.org/10.1021/ie100323d>
- Manenti, F., Pelosato, R., Vallevi, P., Leon-Garzon, A. R., Dotelli, G., Vita, A., Faro, M. Lo, Maggio, G., Pino, L., & Arico, A. S. (2015). Biogas-fed solid oxide fuel cell (SOFC) coupled to tri-reforming process: Modelling and simulation. *International Journal of Hydrogen Energy*, 40(42), 14640–14650. <https://doi.org/10.1016/j.ijhydene.2015.08.055>

- Nestler, F., Schütze, A. R., Ouda, M., Hadrich, M. J., Schaadt, A., Bajohr, S., & Kolb, T. (2020). Kinetic modelling of methanol synthesis over commercial catalysts: A critical assessment. *Chemical Engineering Journal*, 394. <https://doi.org/10.1016/j.cej.2020.124881>
- Nyári, J., Izbassarov, D., Toldy, Á. I., Vuorinen, V., & Santasalo-Aarnio, A. (2022). Choice of the kinetic model significantly affects the outcome of techno-economic assessments of CO₂-based methanol synthesis. *Energy Conversion and Management*, 271. <https://doi.org/10.1016/j.enconman.2022.116200>
- Ojjiagwo, E., Oduoza, C. F., & Emekwuru, N. (2016). Economics of gas to wire technology applied in gas flare management. *Engineering Science and Technology, an International Journal*, 19(4), 2109–2118. <https://doi.org/10.1016/j.jestch.2016.09.012>
- Osat, M., & Shojaati, F. (2022). Assessing performance of methane tri-reforming reactor using a parametric study on the fundamental process variables. *Cleaner Chemical Engineering*, 3, 100050. <https://doi.org/10.1016/j.clce.2022.100050>
- Osman, M., Zaabout, A., Cloete, S., & Amini, S. (2021). Pressurized chemical looping methane reforming to syngas for efficient methanol production: Experimental and process simulation study. *Advances in Applied Energy*, 4. <https://doi.org/10.1016/j.adapen.2021.100069>
- Poto, S., Vico van Berkel, D., Gallucci, F., & Fernanda Neira d'Angelo, M. (2022). Kinetic modelling of the methanol synthesis from CO₂ and H₂ over a CuO/CeO₂/ZrO₂ catalyst: The role of CO₂ and CO hydrogenation. *Chemical Engineering Journal*, 435. <https://doi.org/10.1016/j.cej.2022.134946>
- Pruvost, F., Cloete, S., Hendrik Cloete, J., Dhoke, C., & Zaabout, A. (2022). Techno-Economic assessment of natural gas pyrolysis in molten salts. *Energy Conversion and Management*, 253. <https://doi.org/10.1016/j.enconman.2021.115187>
- Rahmatmand, B., Rahimpour, M. R., & Keshavarz, P. (2019). Introducing a novel process to enhance the syngas conversion to methanol over Cu/ZnO/Al₂O₃ catalyst. *Fuel Processing Technology*, 193, 159–179. <https://doi.org/10.1016/j.fuproc.2019.05.014>

- Ribeiro Domingos, M. E. G., Flórez-Orrego, D., Teles dos Santos, M., de Oliveira, S., & Maréchal, F. (2022). Techno-economic and environmental analysis of methanol and dimethyl ether production from syngas in a kraft pulp process. *Computers and Chemical Engineering*, *163*. <https://doi.org/10.1016/j.compchemeng.2022.107810>
- Santos, R. O. dos, Santos, L. de S., & Prata, D. M. (2018). Simulation and optimization of a methanol synthesis process from different biogas sources. *Journal of Cleaner Production*, *186*, 821–830. <https://doi.org/10.1016/j.jclepro.2018.03.108>
- Sehested, J. (2019). Industrial and scientific directions of methanol catalyst development. In *Journal of Catalysis* (Vol. 371, pp. 368–375). Academic Press Inc. <https://doi.org/10.1016/j.jcat.2019.02.002>
- Soltanieh, M., Zohrabian, A., Gholipour, M. J., & Kalnay, E. (2016). A review of global gas flaring and venting and impact on the environment: Case study of Iran. In *International Journal of Greenhouse Gas Control* (Vol. 49, pp. 488–509). Elsevier Ltd. <https://doi.org/10.1016/j.ijggc.2016.02.010>
- Song, C., & Pan, W. (2004). Tri-reforming of methane: A novel concept for catalytic production of industrially useful synthesis gas with desired H₂/CO ratios. *Catalysis Today*, *98*(4), 463–484. <https://doi.org/10.1016/j.cattod.2004.09.054>
- Stančín, H., Mikulčić, H., Wang, X., & Duić, N. (2020). A review on alternative fuels in future energy system. *Renewable and Sustainable Energy Reviews*, *128*. <https://doi.org/10.1016/j.rser.2020.109927>
- Standard Bank Mozambique, S. B. (2024). *Depósito a Prazo*. <https://doi.org/https://www.standardbank.co.mz/Contas-Cartoes/Contas/Deposito-a-Prazo>
- Sun, D., Li, X., Ji, S., & Cao, L. (2010). Effect of O₂ and H₂O on the tri-reforming of the simulated biogas to syngas over Ni-based SBA-15 catalysts. *Journal of Natural Gas Chemistry*, *19*(4), 369–374. [https://doi.org/10.1016/S1003-9953\(09\)60096-7](https://doi.org/10.1016/S1003-9953(09)60096-7)
- Tahouni, N., Gholami, M., & Panjeshahi, M. H. (2016). Integration of flare gas with fuel gas network in refineries. *Energy*, *111*, 82–91. <https://doi.org/10.1016/j.energy.2016.05.055>

- Tijm, P. J. A., Waller, F. J., & Brown, D. M. (2001). Methanol technology developments for the new millennium. In *Applied Catalysis A: General* (Vol. 221).
- Tomishige, K. (2004). Syngas production from methane reforming with CO₂/H₂O and O₂ over NiO-MgO solid solution catalyst in fluidized bed reactors. *Catalysis Today*, 89(4), 405–418. <https://doi.org/10.1016/j.cattod.2004.01.003>
- Towler, G., & Sinnott, R. (2021). *Principles, practice and economics of plant and process design* (3rd ed.). <https://doi.org/https://doi.org/10.1016/C2019-0-02025-0>
- Wei, J., & Iglesia, E. (2004). Isotopic and kinetic assessment of the mechanism of reactions of CH₄ with CO₂ or H₂O to form synthesis gas and carbon on nickel catalysts. *Journal of Catalysis*, 224(2), 370–383. <https://doi.org/10.1016/j.jcat.2004.02.032>
- Zhang, Y., Cruz, J., Zhang, S., Lou, H. H., & Benson, T. J. (2013). Process simulation and optimization of methanol production coupled to tri-reforming process. *International Journal of Hydrogen Energy*, 38(31), 13617–13630. <https://doi.org/10.1016/j.ijhydene.2013.08.009>

APPENDICES: SUPPLEMENTAL MATERIAL

**APPENDIX A – TOTAL EQUIPMENT ACQUISITION AND OPERATING
COST ESTIMATION**

Table A1 – Total equipment acquisition cost estimation.

Equipment	Year				
	2020	2021	2022	2023	2024
K1	33,150,399	34,300,718	37,034,485	41,145,313	43,531,741
K2	8,287,600	85,75,179	9,258,621	10,286,328	10,882,935
K3	4,056,498	4,197,259	4,531,780	5,034,808	5,326,827
K4	4,322,358	4,472,344	4,828,790	5,364,785	5,675,943
K5	1,423,796	1,473,202	1,590,616	1,767,174	1,869,670
K6	1,048,657	1,085,045	1,171,523	1,301,562	1,377,053
C1	37,718	39,027	42,137	46,814	49,529
C2	214,482	221,924	239,612	266,209	281,649
C3	146,692	151,782	163,879	182,069	192,629
C4	37,004	38,288	41,340	45,929	48,592
C5	453,225	468,952	506,328	562,530	595,157
H1	92,562	95,773	103,407	114,885	121,548
H2	158,313	163,806	176,862	196,493	207,890
H3	1,396,578	1,445,039	1,560,209	1,733,392	1,833,929
Pre-reactor 1	560,768	580,227	626,471	696,009	736,377
Pre-reactor 2	67,293	69,628	75,177	83,522	88,366
Pre-reactor 3	39,253	40,615	43,852	48,720	51,545
TRM reactor	73,335	75,879	81,927	91,021	96,300
MeOH reactor	378,241	391,366	422,558	469,462	496,691
F0	115,396	119,400	128,917	143,226	151,533
F1	200,516	207,474	224,010	248,875	263,309
F2	35,883	37,128	40,087	44,537	47,120
F3	41,490	42,929	46,351	51,496	54,482
DC	506,642	524,222	566,003	628,829	665,301
Total without HEN			US\$ 74,646,118		
Total with HEN			US\$ 82,222,787		

Table A2 – Total operating cost estimation.

Raw materials				
NG	Source	Price (US\$/m ³)	Consumption (m ³ /h)	Cost(US\$/year)
	(EIA, 2024)	0.131	52,390	54,904,720
H ₂ O	Source	Price (US\$/m ³)	Consumption (m ³ /h)	Cost(US\$/year)
	(BR, 2021)	1	52.29	418,320
O ₂	Source	Price (US\$/kg)	Consumption (kg/h)	Cost(US\$/year)
	(CA, 2024)	0.21	12896	21,665,280
Auxiliary services				
Electricity		Price(US\$/kWh)	Consumption (kWh)	Cost (US\$/year)
Heating TRM Reactor		0.08	4,500	2,880,000
Cooling MeOH Reactor	Source: (EDM,		416	266,240
Compressors	2024)		54,043	34,587,520
Utility water		Price (US\$/m ³)	Consumption (m ³ /h)	Cost(US\$/year)
		1	501	4,008,000
Direct labor				
Item		Cost/unit (US\$)	Units	Total Cost (US\$/year)
Control operator		22,500	5	112,500
Plant operator		20,000	8	160,000
Total direct labor				272,500
Inderect labor				81,750
Maintenance				9,082,940
Operating supplies				15,138,232
Laboratory				54,500
Payrool charges				68,125
Property taxes and insurance				3,027,647
Total operating costs with HEN			US\$ 146,455,774	
Total operating costs without HEN			US\$ 213,199,774	

**APPENDIX B – RAW MATERIALS AND PRODUCED METHANOL
PROPERTIES**

Table B1 – Raw materials properties.

Variable	LPFG	HPFG	NG
CH ₄ (mole fraction)	0.7801	0.8592	0.9433
C ₂ H ₆ (mole fraction)	0.0332	0.0223	0.0209
C ₃ H ₈ (mole fraction)	0.0240	0.0131	0.0081
i-C ₄ H ₁₀ (mole fraction)	0.0064	0.0028	0.0021
n-C ₄ H ₁₀ (mole fraction)	0.0076	0.0032	0.0025
i-C ₅ H ₁₂ (mole fraction)	0.0029	0.0011	0.0008
n-C ₅ H ₁₂ (mole fraction)	0.0028	0.0010	0.0005
C ₆ H ₁₄ (mole fraction)	0.0021	0.0004	0.0002
C ₇ H ₁₆ (mole fraction)	0.0028	0.0002	0.0001
C ₈ H ₁₈ (mole fraction)	0.0012	0.0001	0
C ₉ H ₂₀ (mole fraction)	0.0090	0	0
CO (mole fraction)	0	0	0
CO ₂ (mole fraction)	0.0037	0.0002	0
H ₂ (mole fraction)	0	0	0
CH ₃ OH (mole fraction)	0	0	0
H ₂ O (mole fraction)	0	0	0
N ₂ (mole fraction)	0.1334	0.0963	0.0215
Mass density (kg/m ³)	0.8320	0.7501	0.7012
Molecular weight (g/mol)	20.300	18.310	17.110
Specific gravity	0.7007	0.6320	0.5918
Mass HHV (kJ/kg)	43,540	46,510	52,830
Sulfur content (wt%)	0	0	0

Table B2 – Produced methanol properties.

Parameter	Value
CH ₄ (ppm)	21.7
N ₂ (ppm)	4
CO ₂ (ppm)	61
H ₂ O (wt%)	0.0139
H ₂ (ppm)	6
CO (ppm)	1
CH ₃ OH (wt%)	98.5
Molecular weight (g/mol)	31,6
Dew point temperature (°C)	65.5
API gravity	45.8
Gross heating value (kJ/kg)	22,315
Specific gravity	0.8
Mass vapor fraction	0
Dew point pressure (atm)	0.42
Mass density (kg/m ³)	583.6
Pour point (°C)	-102
Flash point (°C)	-108

APPENDIX C – EQUIPMENT DESIGN SPECIFICATIONS

Table C1 – Flash tanks.

Parameter	F3	F1	F2	F0
Liquid volume (m ³)	28.1	36.8	22.3	60.0
Vessel diameter (m)	2.9	3.5	2.1	4.6
Vessel height (m)	4.3	3.8	6.2	3.7
Operating pressure (atm)	1.0	50.0	2.0	1,0
Design temperature (°C)	121.0	121.0	121.0	121.0
Operating temperature (°C)	65.0	50.0	49.6	25.0

Table C2 – Heaters and Coolers.

Parameter	C4	C3	H1	C1	H2	C2	H3	C5
Heat transfer area (m ²)	102.9	278.6	487.3	82.6	931.9	1186.7	4499.5	1442.4
Tube design pressure (kPa)	2492.8	1229.5	760.5	415.8	1208.7	415.8	35.1	35.1
Tube design temperature (°C)	293.9	547.9	192.1	877.8	937.0	477.8	257.0	247.2
Tube operating temperature (°C)	35.0	35.0	164.3	35.0	929.2	35.0	229.2	35.0
Tube outside diameter (mm)	25.4	25.4	25.4	25.4	25.4	25.4	25.4	25.4
Shell design pressure (kPa)	3789.8	1894.9	473.3	243.4	772.0	243.4	53.1	53.1
Shell design temperature (°C)	293.9	547.9	127.8	877.8	917.8	477.8	247.8	247.2
Shell operating temperature (°C)	266.2	520.2	100.0	850.0	890.0	450.0	220.0	219.4
Tube length extended (m)	6.1	6.1	6.1	6.1	6.1	6.1	6.1	6.1

Table C3 – Distillation column.

Parameter	DC
Diameter bottom section (m)	2.6
Bottom tangent to tangent height (m)	39.0
Design gauge pressure bottom (bar)	2.4
Design temperature bottom (°C)	121.1
Operating temperature bottom (°C)	65.5
Number of trays bottom section	58.0
Bottom tray type	Sieve
Bottom tray spacing (m)	0.6

Table C4 – Compressors.

Parameter	K1	K2	K3	K6	K4	K5
Actual gas flow rate inlet (m ³ /h)	19,171.56	242,123.23	10,115.80	39.00	40,625.01	564.19
Design temperature inlet (°C)	150.00	25.00	159.00	45.00	50.00	44.00
Design temperature outlet (°C)	26,617	520.15	220.09	518.02	56.25	518.66
Design pressure outlet (kPa)	3,445.05	1,722.52	4,964.92	4,964.92	5,218.23	4,964.92
Driver power (kW)	8,643.65	37,098.36	4,548.60	8.33	3,548.75	195.61
Specific heat ratio	1.39	1.40	1.39	1.29	1.41	1.35
Compressibility factor inlet	1.00	1.00	1.01	0.99	1.03	1.00
Compressibility factor outlet	1.01	1.00	1.01	1.02	1.03	1.02
Driver type	Motor	Motor	Motor	Motor	Motor	Motor

Table C5 – Methanol reactor.

Parameter	MeOH_reactor
Heat transfer area (m ²)	24,529.7
Tube design pressure (bar)	53.1
Tube design temperature (°C)	247.8
Tube operating temperature (°C)	220.0
Tube outside diameter (m)	0.1
Shell design pressure (bar)	35.1
Shell design temperature (°C)	121.1
Shell operating temperature (°C)	35.0
Tube length extended (m)	12.2

Table C6 – Tri-reforming of methane reactor.

Parameter	TRM_reactor
Vessel diameter (m)	1.22
Vessel height (m)	10.06
Design gauge pressure (kPa)	103.43
Design temperature (°C)	877.78
Operating temperature (°C)	850.00
Total packing height (m)	9.75

Table C7 – Pre-reactors.

Parameter	Pre-reactor 1	Pre-reactor 2	Pre-reactor 3
Vessel diameter (m)	0.75	0.75	0.75
Vessel height (m)	1.13	1.13	1.13
Tank volume (m ³)	0.50	0.50	0.50
Vessel pressure (atm)	1.00	1.00	1.00
Feed temperature (°C)	25.00	25.00	25.00
Flue gas temperature (°C)	999.00	1,665.00	1,270.00